Spatiotemporal transcriptional networks control the plasticity of chickpea root exodermis

Authors: Leonardo Jo[1,2], Rianne Kluck[1], Sara Buti[1], Julia Holbein[3], Martin Rázus[1], Himanshu Chhillar[4], Pingtao Ding[4], Rochus Benni Franke[3], Kaisa Kajala[1]*

[1] Experimental & Computational Plant Development, Institute of Environmental Biology, Utrecht University, Utrecht, the Netherlands

[2] Current Affiliation: Laboratory of Molecular Biology, Wageningen University & Research, Droevendaalsesteeg 1, 6708PB, Wageningen, The Netherlands.

[3] Institute of Cellular and Molecular Botany, Rheinische Friedrich-Wilhelms-University of Bonn, Bonn, Germany.

[4] Institute of Biology Leiden, Leiden University, Leiden, the Netherlands.

* Corresponding author, k.kajala@uu.nl

Abstract

Abscisic acid (ABA) regulates plant responses to stress and influences the differentiation of root barrier cell types, such as the endodermis and exodermis. Despite the importance of the exodermis in limiting water and solute fluxes, its regulation remains poorly understood in legumes. Here, we characterize the ABA-induced suberization and lignification of root tissues across eight galegoid legumes to identify exodermis-forming species in the clade. Chickpea deposited suberin lamella specifically in the outermost cortex and formed a functional apoplastic barrier, i.e. an exodermis. Transcriptomics of chickpea roots revealed ABA-induced programs that were temporally separated, specifically, a rapid program with the general ABA response, and a delayed programs of suberin and lignin biosynthesis. We identified WRKY and MYB transcription factors that putatively link the ABA response to the suberin biosynthesis, and using single-cell RNA-seq of chickpea roots we inferred an exodermis-expressed WRKY-MYB regulatory unit upstream of the suberin biosynthetic genes. Transactivation assays supported an ABA-dependent transcription factor activity upstream of suberin biosynthesis pathway in chickpea. Our results reveal a cell-type specific transcription factor hierarchy that coordinates hormone perception into an important mechanism of root plasticity in legumes.

Plants exhibit indeterminate and highly plastic growth, allowing them to adjust their development in response to fluctuating environmental conditions. This plasticity extends to the differentiation trajectories of individual plant cells, which are not solely determined by developmental programs but also integrate environmental signals to modify their structure and function. One of the key stress cues in plants is abscisic acid (ABA), a plant hormone that regulates many responses to drought, salinity, and other abiotic stressors. ABA has been shown to influence the differentiation of various root cell types, including the endodermis and the exodermis. In these barrier cell types, ABA induces a differentiation program that deposits suberin into the cell wall[1–5]. Suberin deposition significantly contributes to the apoplastic diffusion barrier properties of these cell types and help with retention of water and likely oxygen[3,5,6]. Notably, endodermis and exodermis also have another differentiation program that deposits localized lignin into their cell walls, and this program is in many species under developmental control[7–14]. The endodermal lignin is precisely positioned and forms the Casparian strip that divides the endodermal cells to soil-

facing and vasculature-facing sides and functions as an apoplastic diffusion barrier between the two. This provides the endodermis the ability to be a selective control point for two-way fluxes between the root and the soil[15]. Together, the endodermis and the exodermis coordinate their critical roles in regulating the two-way fluxes of water, solutes and gases and protecting plants against environmental stressors. At the same time, they each integrate numerous environmental cues into their differentiation programs to optimize their functions.

While the endodermis is one of the best characterized plant cell types for its development and differentiation[16,17], the exodermis remains relatively unexplored because the model for root development, *Arabidopsis thaliana*, lacks this cell type[18]. However, the exodermis in its diverse morphologies is found in around 90% of flowering plants[19–21]. Considering the ABA-induced differentiation program in endodermis and exodermis, there is diversity also in its regulation across the flowering plants but universally, the suberin deposition program is regulated by a group of closely related MYB (MYELOBLASTOSIS) transcription factors (TFs)[22,23]. In Arabidopsis, ABA induces the deposition of endodermal SL via multiple, redundantly acting MYBs from clades S10, S11 and S24[24,25] including AtMYB39, AtMYB41, AtMYB53, AtMYB92 and AtMYB93[2,26,27]. Similarly in rice, four MYBs, OsMYB39a, OsMYB41, OsMYB92a, and OsMYB92b, were identified as the redundant core regulators of endodermal suberin, which also were responsive to ABA[4]. Intriguingly, these rice MYB TFs do not affect the exodermal suberin which also are deposited in rice roots in response to ABA, suggesting that a separate set or additional TFs are required for exodermal suberin in rice. In contrast, tomato has suberin only in the exodermis and the homologs of these MYBs, specifically SlMYB92, SlMYB41 and SlMYB63, regulate the exodermal SL in a non-redundant fashion[3,28]. So, a set of conserved MYBs regulates the suberin differentiation program, which is ABA-responsive in endodermis, exodermis, or both, depending on the angiosperm species. In addition to MYBs, suberin biosynthesis is also regulated by some of the WRKY family TFs. Specifically, AtWRKY9[29] and AtWRKY33[30] directly induce expression of Cytochrome P450 genes (*CYPs*) encoding AtCYP94s and AtCYP86s that carry out fatty acid ω-oxidation in suberin biosynthesis[31]. In tomato, SlWRKY71 was shown act antagonistically to SlMYB93 and SlMYB41, and repress expression of suberin biosynthesis genes[28]. Ultimately, the direct link between ABA signalling and these cell-type-specific differentiation programs coordinated by the MYBs and WRKYs remains unknown.

Exodermis has been reported to be found in the majority of angiosperm families, with only a small number of families having species either with and without an exodermis[19–21,32]. Legumes (Fabaceae) were originally reported as one of the families not containing species with an exodermis[19] and it was hypothesized that the presence of a barrier at the outermost cortex layer would be inhibitory to the legumes' ability to form symbioses with nitrogen-fixing bacteria in root nodules formed from the cortex layer[33]. In the past two decades there has been contrasting reports of the presence of exodermis in different legumes such as pea (*Lathyrus oleraceus*, previously *Pisum sativum*)[19,34,35] and chickpea (*Cicer arietinum)*[36,37], and this may be due to the stress-induced, dynamic nature of the exodermis in many species. Intrigued by this gap of knowledge and potential diversity of root barriers in legumes, we set out to characterize the ABA-responsive differentiation programs in a selection of galegoid legumes such as chickpea, lentil and alfalfa to query how exodermis is regulated in this clade. Our results provide key insights into the diversity of cell-type specific responses to ABA across legume species and identify core components of the regulatory network that translate hormone perception into exodermis differentiation in chickpea.

Results

Galegoid legumes have diverse root barrier phenotypes

To investigate the root suberization and lignification in galegoid legumes and the effect of ABA on it, we grew eight species selected based on previous reports of exodermis in legumes [19,34–37] in the

presence or absence of 2 μM ABA (Fig. 1a). After 3 days, root cross-sections of the middle region of the root (50% region) were stained with Fluorol Yellow (FY) and Basic Fuchsin (BF), fluorescent dyes that bind to suberin and lignin, respectively[38–41], and the fluorescence intensity of the cell wall was quantified across individual cell layers (Figure 1b). Based on this histochemical screen, ABA induced suberization and lignification in distinct root cell layers across the galegoid clade (Fig. 1c, Extended Data Fig. 1, Supplementary Fig. 1). In chickpea and *L. oleraceus*, ABA promoted suberin accumulation specifically in the outermost cortical cell layer (C1) and not in the endodermis (EN), indicating presence of an exodermis in these species. In contrast, ABA induced the suberization of the endodermis in *Lens culinaris* (lentil), *Medicago truncatula* (barrel medic), *Medicago sativa* (alfalfa), and *Trifolium repens* (white clover), with a weak FY and BF signal observed in cortical cell layers. *Vicia sativa* (common vetch) displayed a unique pattern of FY staining in multiple outer layers of the root cortex as well as in the endodermis in response to ABA. In *Lotus japonicus* (narrowleaf trefoil), the process of root suberization in the endodermis occurred independently of ABA at the sampled developmental stage, and indeed the root zone affected the number of suberized cells across species (Supplementary Fig. 2).

<u>Chickpea forms a functional exodermal barrier in response to ABA</u>

Suberin monomer profiling further confirmed that ABA promotes the accumulation of suberin monomers in chickpea, *M. truncatula*, and *V. sativa* (Fig. 2a, b, Supplementary Table 1), with the overall increase of *cis*- and *trans*-ferulic acid, long-chain fatty acids (C18, C20, C22), α-ω-diacids (C16, C18:1, C18) and ω-hydroxy acids (C16, C18:1 and C22) (Extended Data Fig. 2a). Given these diverse patterns of suberin accumulation, we examined the ultrastructure of the suberin in C1 layer (Fig. 2c) and endodermis (Extended Data Fig. 2b) using transmission electron microscopy (TEM) for three species with contrasting FY phenotypes. In chickpea roots grown in the presence of ABA, C1 displayed a clear suberin lamella (SL), characterized by a pattern of alternating dark and light bands[42] (Fig. 2c). In contrast, while the SL was clearly present in the endodermal cell layer of *M. truncatula* and *V. sativa* (Extended Data Fig. 2b), it was absent in the C1 cells in these species (Fig. 2c). Despite the high FY signal detected in the outer cortex of *V. sativa* (Fig. 1c), TEM revealed an amorphous suberin structure lacking the alternating banding pattern typical for SL.

To determine if ABA-induced compounds in the cortex of these species function as an apoplastic diffusion barrier, we tested if they restrict the diffusion of propidium iodide (PI)[7,8]. PI apoplastic diffusion was blocked in chickpea roots treated with ABA as indicated by the lack of PI fluorescent signal in inner cortical cell layers when compared to mock-treated roots (Fig. 2d). This suggests that ABA-induced cell-type-specific modifications in the cell wall of C1 results in the establishment of a functional apoplastic barrier in chickpea. This supports the chickpea C1 being a functional exodermis. However, as chickpea exodermis has both SL and lignin in response to ABA, we cannot determine which one(s) provide the apoplastic barrier function. Previous work supports lignin, the main component of the Casparian strip, critical for blocking apoplastic diffusion of PI[8,14]. In *M. truncatula* and *V. sativa*, PI diffused into the inner cortex layers in both mock and ABA-treated roots (Fig. 2d). The cortex layers with FY and BF signal also resulted in strong PI signal in chickpea and *V. sativa* (Fig. 1d and 2e), which may relate to cross-reactiveness of PI with the cell wall modifications. In summary, our results demonstrate that the stress hormone ABA promotes suberin and lignin accumulation in the outer cortex of various legume species. Specifically, chickpea exhibited a robust single-layer response with deposition of structured SL and lignin and forming a functional apoplastic diffusion barrier, i.e., an exodermis.

<u>ABA-induced transcriptome changes specify temporally and functionally distinct expression modules in chickpea roots</u>

The suberin biosynthesis and deposition pathway is a coordinated process with many enzymes that operate in different cellular compartments[31] (Fig. 3a). To understand how the process of ABA-induced exodermal differentiation leading to apoplastic barrier formation is transcriptionally

regulated, we profiled the chickpea root transcriptome at nine different timepoints: 15, 30 and 45 minutes, and 1h, 2h, 4h, 6h, 8h and 24h after mock or ABA exposure (Fig. 3b, Supplementary Table 2). ABA induced primarily upregulation of gene expression (Fig. 3c). K-means clustering of differentially expressed genes (DEGs) identified temporal expression patterns in response to ABA (Fig. 3d, Extended Data Fig. 3a, Supplementary Table 2). Genes exhibiting a rapid upregulation (30 to 1 hour) were grouped into Modules I, II and III ("early"), while Modules IV, V and VI represented temporally delayed transcriptional responses showing continuous upregulation of genes from 2h or later ("late", Fig. 3d). Genes involved with the canonical ABA response, like members of Clade A *PROTEIN PHOSPHATASE TYPE 2C* (*PP2C*), *RESPONSIVE TO DESICCATION 29* (*RD29*), and *LATE EMBRYOGENESIS ABUNDANT* (*LEA*) were found in the early modules (Fig. 3c, Extended Data Fig. 3b). In contrast, suberin biosynthesis and deposition genes (Fig. 3a), were found in the late modules (Fig. 3c, Extended Data Fig. 3c). Matching the transcriptional timing, suberin accumulation in the exodermis could be detected by FY after 24h (Supplementary Fig. 3). Contrastingly, lignin biosynthesis and deposition genes were found in both early (II, III) and late (V, VI) clusters (Extended Data Fig. 3d, e). In summary, the expression of suberin biosynthesis genes is temporally separated from genes in the general ABA response in chickpea roots, while lignin overlaps with both, indicating separate regulatory mechanisms.

To understand the transcriptional regulatory mechanisms underlying the temporal separation between the general ABA response and the suberin biosynthesis program, we analysed the DNA *cis*-element composition of promoters (500 base pairs upstream the coding sequence) of genes belonging to modules I-VI (Fig. 4a, b, c, Extended Data Fig. 4). Motif enrichment analysis revealed that the G-box *cis*-element (CACGTG), the main DNA element targeted by the canonical ABA response[43,44] was significantly enriched only in the promoters of the early modules (Fig. 4a). This supports the rapid transcriptional response observed in chickpea roots occurring through the canonical ABA signalling pathway[45]. We observed other *cis*-elements enriched in the promoters of late modules, including that of suberin-regulating MYB41 TF (ACCTA)[23,46,47] (Fig. 4b) and WRKY40 (TTGACT)[47] (Fig. 4c). This indicates that albeit ABA-induced, suberin biosynthesis in the chickpea exodermis is not directly controlled by the canonical ABA signalling pathway. Instead, it appears to be regulated through ABA-induced changes in the regulatory state of exodermal cells, with the involvement of other TFs, like MYBs and WRKYs, that control the temporally separated expression of suberin biosynthesis genes.

Based on these results, we hypothesized that ABA enhances the expression and/or activity of specific MYB and WRKY TFs through the canonical ABA signalling pathway. These TFs, in turn, initiate the suberin biosynthesis program in chickpea roots. Among the ABA-induced *MYBs* and *WRKYs*, *Ca_00232, Ca_14119* (Fig. 4d), and *Ca_01018* (Fig. 4e) were rapidly upregulated within 45 minutes of ABA exposure a pace similar to *Ca_01548*, an *AREB* (*ABA RESPONSIVE ELEMENTS-BINDING PROTEIN*) and an indicator of the canonical ABA response (Fig. 4f). Phylogenetic analysis revealed that Ca_00232 shares a close evolutionary relationship with AtMYB74 and AtMYB102 and Ca_14119 with AtMYB41 (Supplementary Fig. 4a). In Arabidopsis, these MYB TFs have been characterized as direct targets of the ABA signalling, and AtMYB41 regulates the suberization of the root endodermis[1,2,26,48,49]. For the WRKY Ca_01018, the closest homologs were AtWRKY23 and AtWRKY68 (Supplementary Fig. 4b). Other *MYB* and *WRKY* DEGs presented a later response to ABA in a similar temporal pattern as the expression of suberin biosynthesis genes (Fig. 4d, e, Extended Data Fig. 3c), and some of these, e.g. *Ca_11228*, *Ca_11494* and *Ca_11832*, are close orthologues of known regulators of suberin, such as Arabidopsis *SUBERMAN* (*AtMYB39*)[27] (Supplementary Fig. 4a, Fig. 4d).

<u>Exodermis-specificity is progressively enriched in the ABA-induced transcriptome</u>

As suberin deposition in response to ABA is highly exodermis-specific in chickpea seedling roots, we next profiled the single cell transcriptome of chickpea roots treated with ABA to infer spatial expression patterns. We profiled the transcriptome of over 10,000 protoplasts isolated from ABA-

treated roots (Extended Data Fig. 5a) and detected 8,639 high-quality cells in our dataset which formed 22 UMAP clusters with representative marker genes (Fig. 5a). We considered marker genes to have expression in at least 20% of cells of the marked cluster, a percentage difference of at least 20% to other clusters, an average logFC greater than 1, and an adjusted P-value lower than 0.01 (Fig. 5b, Supplementary Table 3). Similar cell-type clusters and markers were observed in another independent experiment (Supplementary Fig. 5). To identify the representative cell type identity of the clusters, we compared if orthologues of marker genes were characterized as marker genes in the *Arabidopsis* scRNA-seq root database scPlantDB (Supplementary Fig. 6)[50]. For instance, the meristematic cell and the endodermis cortex initials (ECi) clusters showed high similarities to cell division markers clusters in the scPlantDB (meristematic cell, G1/G0 phase, G2/M phase and S phase) (Fig. 5b, Supplementary Fig. 6a). Half of our xylem cell cluster marker genes had an orthologue annotated as a marker for xylem (47%) or metaxylem (56%) clusters in Arabidopsis (Supplementary Fig. 6b). We further analysed the expression of empirically determined root cell markers in Arabidopsis[51] to refine the annotation of individual clusters, including cortex, phloem and epidermis (Supplementary Fig. 7). Altogether, this approach allowed us to identify the cell types that the 22 UMAP cluster likely correspond to (Fig. 5a, b).

In accordance with what we observed at the cellular level (Fig. 5c, d), our single cell transcriptome data revealed a separation between the transcriptional programs for Casparian strip development and for suberization into different clusters (Fig. 5e). The orthologs of the genes involved in Casparian strip formation were exclusively expressed in the endodermal cluster (Fig. 5f), including *GASSHO1/SCHENGEN3* (*SGN3*), *CASPARIAN STRIP MEMBRANE PROTEINs* (*CASPs*) and their regulator *MYB36*[9,52,53]. Additionally, the Casparian strip formation in Arabidopsis requires the stele-produced peptide CASPARIAN STRIP INTEGRITY FACTOR1 (CIF1)[12,13]. We observed that also in chickpea, the closest orthologue to *AtCIF1* (*Ca_20263*) was highly expressed in stele cell clusters (Pericycle 1 to 3, Phloem1 and Stele Initials) (Fig. 5e). Then, to identify the exodermis cells that do not exist in Arabidopsis, we used the expression of suberin biosynthesis genes. Among them, we identified one *CaASFT1* (*Ca_26067*), two *CYP86s* (*CaCYP86A1*: *Ca_15610*; *CaCYB86B1*: *Ca_11097*), two *KCSs* (*CaKCS1*: *Ca_01346*; *CaKCS11*: *Ca_12147*); one *ABCG* (*CaABCG23*: *Ca_21808*), four *GPATs* (*CaGPAT1*: *Ca_15259, CaGPAT5*: *Ca_16115, CaGPAT6*: *Ca_25903* and *CaGPAT8*: *Ca_13742*) and two *GELPs* (*CaGELPa*: *Ca_09232*; *CaGELPb*: *Ca_24203*) to be mainly expressed in the exodermis cluster (Fig. 5e). Overall, these annotated cell clusters provide an atlas of cell types of the chickpea root and offer valuable insights into the molecular mechanisms of root cell-type-specific responses to ABA.

Next, we queried the expression of the ABA-induced DEGs from the time-course experiment (Fig. 4) in our single cell data clusters (Supplementary Fig. 8, 9). We observed that genes from the early response (modules I-III, Fig. 3d) were typically expressed in multiple clusters and throughout the different single cell clusters of the chickpea root (Supplementary Fig. 8), while the genes belonging to the late response (modules IV-VI, Fig. 3d) were primarily expressed in the exodermis cell cluster (Supplementary Fig. 9). We wanted to test if the ABA-responsive modules (I-III) were enriched in genes expressed only in specific cell types. Hence, we tested if genes identified in temporal modules were enriched in the list of cell-specific gene markers (Fig. 3f, Supplementary Table 3), which revealed that early modules II and III were highly enriched in many different cell clusters, including the exodermis-cluster (Fig. 3f). However, the late modules IV and V were enriched primarily in the exodermis cell cluster (Fig. 3f). Thus, the strong transcriptional response to ABA in the exodermis likely reflects the unique ability of these cells to promote the expression of genes involved with suberin and lignin biosynthesis and deposition pathways in response to ABA.

Finally, we mapped the expression of ABA-induced lignin biosynthesis genes in the single cell data and observed expression in multiple clusters, especially those representing the cell types that use lignin in their secondary cell walls: exodermis, endodermis and xylem (Extended Data Fig. 5b, Extended Data Fig. 1, Fig. 5c). The lignin biosynthesis genes belonging to module II were

expressed in both clusters representing endodermis and exodermis (Extended Data Fig. 5b). Both the expression pattern and the earlier induction from suberin biosynthesis genes indicates separate regulatory mechanisms for the two biosynthesis units. Lignin is also known to be regulated by MYB TFs[54], so we queried the closest homologs of known lignin-regulating MYBs (Extended Data Fig. 5c-f) in our data. None of them were induced by ABA, but *Ca_12226* and *Ca_22597*, homologs of *AtMYB58* and *AtMYB63* encoding for positive regulators of lignin[55], were expressed in some of the cells of the exodermis cluster (Extended Data Fig. 5b).

Temporal and developmental trajectories of *MYB* and *WRKY* TFs align

Then, we queried the expression of *MYBs*, *WRKYs* and *AREB* DEGs identified in the time-course experiment (Fig. 4d-f, 5e). In accordance to the general trends for early and late modules, we observed that TF genes from the early clusters, including *Ca_00232 (CaMYB74/102), Ca_14119 (CaMYB41)*, *Ca_17479* (*CaMYB37/38)* and *Ca_01018* (*CaWRKY23/68*) were significantly expressed in the exodermis cluster, but also in clusters representing cell types overlaying exodermis (rootcap and trichoblast clusters) (Fig. 5e), while genes from the late modules, such as *Ca_11228* (*CaMYB9/107*) and *Ca_06163* (*CaWRKY43),* were specific to the exodermis cluster (Fig. 5e). Altogether, these data may indicate a hierarchical cascade of ABA-induced TFs, where the downstream TFs are restricted into one cell type, the exodermis, to induce suberin biosynthesis in cell-type specific manner in the chickpea root. Since we observed that many of the suberin biosynthesis genes to be solely expressed in the exodermis cluster, we propose that chickpea exodermis is uniquely specialized to translate the ABA-mediated changes in the regulatory landscape into the activation of the suberin biosynthesis program.

To reconstruct the spatial and temporal dynamics of ABA-induced suberization in the exodermis, we utilized the Slingshot package[56] to infer developmental trajectories of outer cortex and exodermis cells (Fig. 6a). Unsupervised lineage detection revealed two main lineages starting from the Meristem_1 cluster, lineage 1 to Exodermis_1 and lineage 2 to OuterCortex_2, both via OuterCortex_1 (Fig. 6a, b, Extended Data Fig. 6a). Pseudotime estimation in lineage 1 revealed that the expression of suberin biosynthesis gene expression initiated late in the exodermal developmental trajectory (Fig. 6c), while they were not expressed in lineage 2 (Extended Data Fig. 6b). This reflects the ABA-induced temporal expression changes combined with the developmental trajectory along the root in chickpea (Supplementary Fig. 2). When looking at the expression of TFs along the pseudotime trajectory, we observed that the majority of *MYBs* upregulated by ABA showed expression patterns similar to the suberin biosynthesis genes (Fig. 6c). However, similarly to the time-course data (Fig. 4e, f), *CaMYB74/102 (Ca_00232)* and *CaWRKY23/68* (*Ca_01018)* showed early expression patterns along the exodermal lineage trajectory (Fig. 6d). Thus, our single-cell analysis led us to hypothesise a role for CaMYB74/102 (Ca_00232) and CaWRKY23/68 (Ca_01018) as links between the early ABA perception and the delayed spatial control of suberin biosynthesis in the chickpea root exodermis.

CaWRKY23/68 is a putative link between ABA response and suberin regulation

To test our hypothesis, we used a trans-activation assay in *Nicotiana benthamiana* leaves (Fig. 6d). In this assay, we tested three hypotheses. Firstly, we tested if an ABA treatment in this orthologous system was able to induce expression of our target genes (Fig. 6e). In addition to *CaMYB74/102* (*Ca_00232*) and *CaWRKY23/68* (*Ca_01018*) promoters, we also tested those of *CaMYB9/107* (*Ca_11228*), *CaMYB41* (*Ca_14119*) and two ABA-induced, exodermis-specific suberin biosynthesis genes (*CaCYP86B1* (*Ca_11077*) and *CaGPAT5* (*Ca_16115*)). We observed a mild induction of only *pCaWRKY23/68* in response to ABA in the YFP control (Fig. 6e), which supports its role as a downstream target of canonical ABA signalling. Secondly, we tested if our candidate TFs, CaMYB74/102, CaWRKY23/68, CaMYB41 or CaMYB9/107, could induce expression of each other in the presence or absence of ABA. CaWRKY23/68 induced the expression of *CaMYB74/102* and *CaMYB9/107*, but only in the presence of ABA application (Fig. 6e). This indicates a post-translational effect on CaWRKY23/68 activity by ABA signalling, either

by a direct modification such as phosphorylation[57], or by presence of required cofactors. Additionally, expression from *pCaMYB9/107* was induced by all tested TFs, but again, only in the presence of ABA (Fig. 6e). This activation of *pCaMYB9/107* by multiple TFs indicates it is downstream from the other TFs which is in agreement with its late expression in both the time-course (Fig. 4d) and the pseudotime trajectory (Fig. 6c), but at odds with its exodermis-specific expression (Fig. 5e). In our profiled cells, only cells in the exodermis cell-cluster express both *CaMYB9/107* and its putative upstream TFs (Supplementary Fig. S10), so a permissive regulation and self-induction may be employed to amplify transient signals and enforce suberin biosynthesis in response to ABA (Fig. 6e). Finally, we tested if our candidate TFs can activate genes in the chickpea suberin biosynthesis pathway. All tested CaMYBs were able to drive expression from *pCaCYP86B1* and *pCaGPAT5* both in the presence and absence of ABA treatment (Fig. 6e). This allowed us to propose a gene regulatory network linking ABA to suberin biosynthesis via CaWRKY23/68 transcriptional and post-translational activation and the downstream activation of suberin-related and exodermis expressing MYB TFs (Fig. 6f).

Discussion

Our characterization of ABA-induced deposition of cell wall polymers in galegoid legume cortical layers uncovered diversity of phenotypes representing diverse differentiation trajectories (Fig. 1, Extended Data Fig. 1). We resolved some previous unclarities of presence of exodermis, e.g. in pea[34,35], to be due to ABA-mediated, i.e. environmental, induction of suberin and lignin. For chickpea, we show that the differentiated exodermis with SL (Fig. 2c) and non-polar lignin deposition (Extended Data Fig. 1) acts as a functional apoplastic barrier (Fig. 2d). Given the infrequent occurrence of exodermis in the legume clade, chickpea represents a novel model for this cell type that provides additional resilience traits against environmental stressors[3,36].

We also observed one species, *V. sativa*, where strong FY and BF signal in multiple outermost cortical layers (Fig. 1, Extended Data Fig. 1) did not correlate with presence of SL (Fig. 2c) or apoplastic barrier to PI diffusion (Fig. 2d). While SL was not observed in *V. sativa*, we hypothesize that the compounds detected by the FY histochemical assay are related to suberin, possibly its monomers unable to polymerize. It may be that *V. sativa* represents either a mutation in one of the key biosynthesis or polymerisation enzymes, or a snapshot of suberin deposition pathway evolution, i.e. loss or gain of the complete set of enzymes and transporters needed. Discovery of this intermediate phenotype between presence and absence of exodermis will provide opportunities for research of root barrier evolution.

Transcriptional investigation of the chickpea exodermis differentiation trajectory with time-course and single cell approaches revealed a group of WRKY and MYB TFs that putatively connect general ABA signalling with exodermis-specific suberization (Fig. 6f). Certain WRKY[28–30] and MYB[1–3,22,23,26,27] family TFs are known for their roles in regulating suberin deposition. Similarly to tomato[3,28,58], we identified MYB TFs that induce suberin biosynthesis genes (Fig. 6e) expressed in the cluster representing exodermis and not the endodermis (Fig. 5e). However, the CaWRKY23/68 we identified as the top-tier transcriptional activator of *CaMYB74/102* and *CaMYB9/107* (Fig. 6e, f) plays a different role than the previously identified suberin-regulating WRKYs. In Arabidopsis, AtWRKY9 and AtWRKY33 directly bind the promoters of *CYP* genes of the suberin biosynthetic pathway[29,30], while we did not observe CaWRKY23/68 activating the ABA-induced exodermis-specific *CaCYP8B1 (Ca_11097)*. In tomato, SlWRKY71 works antagonistically to suberin-inducing MYBs[28], repressing the expression of suberin biosynthesis genes. We observed no effect of CaWRKY23/68 onto the suberin biosynthesis genes (Fig, 6e) but detected a small repression of *pCaWRKY23/68* promoter activity by the suberin-inducing MYBs (Fig, 6e). This observation indicates that there is negative feedback between WRKYs and MYBs in chickpea (Fig. 6e) and tomato[28], even though working at different levels in the gene regulatory network.

Although ABA is widely known as a suberin inducing signal acting via induction of the suberin-regulating MYBs[1–3,49,59], the molecular mechanism how ABA triggers their induction has remained

elusive. We observed that the TF activity of our top-tier TF, CaWRKY23/68, was induced by ABA in the transactivation assay (Fig. 6e), which could serve as such a mechanism. The activation is likely a post-translational effect as the TFs were expressed under a strong near-constitutive promoter. WRKY TF activity is commonly strengthened by phosphorylation in Arabidopsis[60,61], and CaWRKY23/68 is predicted to have four phosphorylation sites (Extended Data Fig. 6c)[62], making phosphorylation a good candidate for an induction mechanism. Furthermore, rice WRKY72 has been shown to be phosphorylated in response to ABA by the canonical ABA signaling component SnRK2 (SNF1-related protein kinase 2)[63,64]. It remains to be queried if WRKYs and their phosphorylation is the bridge between ABA perception and the canonical regulation of suberin by MYBs in various model systems.

It is not known how exodermis cell identity is positionally specified in any species, and similarly, our data did not allow identification of the cue that restricts the expression of *CaMYB9/107* and suberin biosynthesis genes specifically to the exodermis cluster (Fig. 5e). Expression of the early TFs, *CaWRKY23/68, CaMYB74/102* and *CaMYB41,* had wider domains, i.e. they were also expressed in clusters representing cell types overlaying the exodermis (root cap, trichoblast, Fig. 5e), which indicates restriction of the expression pattern along the progression of the network hierarchy and suggesting that the spatial or exodermis-identity cue does not necessarily act at the top level of this network module. However, we cannot exclude the possibility that our experimental setup using exogenous ABA as the exodermis differentiation cue may have expanded the expression domains of the early TFs. ABA is made in response to environmental stresses, such as drought or salinity, and recently, it was shown that in rice, compaction-responsive ABA originates from internal tissues such as phloem[65]. Hence, the expression domains may be affected by the unusual direction or concentration of ABA, and further research would be needed to resolve if the wide expression patterns we observe for the early TFs (Fig. 6f) would be also observed in endogenous ABA-inducing abiotic stresses. Overall, our data provide evidence of functional sufficiency of the WRKY/MYB transcriptional module in the activation of the suberin biosynthesis program in chickpea exodermis, and how the expression pattern of this module is restricted to exodermis remains an exciting avenue for future research.

In addition to suberin gene expression unit in chickpea exodermis, there is also a lignin unit. We observed lignin biosynthesis genes be expressed temporally in both early and late modules (Extended Data Fig. 6d, e), supporting lignin regulatory unit being distinct from the suberin unit. Our data did not support clear candidates as regulators of lignin biosynthesis in exodermis (Extended Data Fig. 4, 5) but similar questions remain as for regulation of suberin biosynthesis. What sets exodermis apart from the other cell types in its gene regulatory capacity to induce lignin biosynthesis? What are the ABA-induced changes, possibly post-translational, that form the exodermis-specific, ABA-induced lignin biosynthesis unit?

All in all, we characterized the barrier occurrence and characteristics in several galegoid legumes, providing the first comparative framework for understanding root barrier diversity and evolution in this clade. Our characterization of temporal and spatial gene expression patterns in chickpea in response to ABA reveals key regulatory modules associated with hormone perception and cell-type specific suberin deposition in the legume family. Looking ahead, comparative transcriptomic analyses across the galegoid family will be crucial for uncovering the evolutionary innovations underlying the phenotypic diversity we observed. The conservation and divergence of temporal and spatial gene expression patterns (Fig. 3d, 5a, 6c) and the regulatory interactions observed in chickpea (Fig. 6e, f) remains to be tested in non-exodermal galegoid legumes, and thus, will provide important insights into how legume root barriers have evolved.

Online methods

Sterilization and germination of legume seeds

Legume seeds were obtained from the following sources: *C. arietinum* Anigiri accession ICC 5679 from ICRISAT; *L. oleraceus* Cameor[66] from Judith Boursin, *L. culinaris* Groene Dupuis and *V. sativa* Prontivesa from Vreeken's Zaden (the Netherlands), *L. japonicus* Gifu from Tonni Andersen, *M. truncatula* A17 from Wouter Kohlen, and *M. sativa* and *T. repens* from Intratuin B.V. (the Netherlands).

Seeds from *C. arietinum* Anigiri, *L. oleraceus* Cameor, *L. culinaris* Groene Dupuis, *V. sativa* Prontivesa, *T. repens,* and *M. sativa* were gas sterilized by placing the seeds in a desiccator with a mixture of 50 mL of commercial bleach and 2.5 mL of HCl for 12 hours. After sterilization, seeds were soaked in distilled water for 12 hours in the dark at room temperature. Soaked seeds were placed onto sterile 0.7% (w/v) Phytoagar (Duchefa) dissolved in water. Seeds were then germinated in the dark for 3 days at 25°C. For the germination, plates were kept in a 60° to 70° angle to ensure a uniform growth direction of the roots. For *M. truncatula* A17, seeds were scarified for 7 minutes using sulfuric acid and sterilized for 7 minutes with 10% (v/v) commercial bleach. After sterilization, the seeds were washed five times with distilled water and kept in water for 12 hours. After soaking, seeds were placed on petri dishes containing 1% (w/v) Phytoagar and cold stratified in the dark at 4°C for three days. To initiate germination, the petri dishes were inverted horizontally (with the medium on top) and transferred to growth cabinets at 25°C in the dark for 12 hours. Germinated seedlings were then transferred to 0.7% (w/v) Phytoagar plates and kept in the dark for another 36 hours in a 60° to 70° standing angle. For *L. japonicus* Gifu, seeds were mechanically scarified with sandpaper and surface sterilized with 10% commercial bleach for 10 minutes. After sterilization, seeds were washed five times and soaked in water at room temperature for 12 hours. Seeds were then transferred to plates with 1% (w/v) Phytoagar and cold-stratified at 4°C in darkness for 3 days. Seeds were germinated at 25°C in darkness for five days and plates were placed in 60-70° angle.

Suberin and lignin histology and fluorescent signal quantification

Four-day old seedlings of, *C. arietinum* Anigiri, *P. sativum* Cameor, *L. culinaris* Groene Dupuis, *V. sativa* Prontivesa, *T. repens* and *M. sativa*, two-day old seedlings from *M. truncatula* A17, and five-day old seedlings from *L. japonicus* Gifu were transferred to ½ MS square plates supplemented with 2 µM ABA or mock conditions. The seedlings were maintained in a D-root system[67] in growth chamber under long-day conditions (16 h light, 8 h dark; 25°C; 70% humidity). After 3 days, 1-cm root segments at the middle point of the root (50% region) were vacuum-infiltrated for 1 h in a solution containing 4% (w/v) paraformaldehyde (PFA) dissolved in PBS buffer. After vacuum infiltration, roots were kept in 4% PFA for at least 12 hours at 4°C and subsequently washed three times with PBS. Root segments were embedded in 4% (w/v) agarose (*C. arietinum*, *P. sativum*, *L. culinaris*, *V. sativa*) or 3% (w/v) (*M. truncatula*, *M. sativa*, *L. japonicus*, *T. repens*) and cross-sectioned into 250 µm thick sections using the VT1000 S vibratome (Leica). Fluorescent staining and confocal imaging of suberin with Fluorol Yellow (FY) and lignin with Basic Fuchsin (BF) in root cross sections was performed as described previously[28]. The quantification of FY and BF fluorescent signals along individual cell layers of the root were done using the Icy software (https://icy.bioimageanalysis.org/). To analyse fluorescence intensity, 2D polylines were manually traced along the anticlinal cell walls of at least 10 individual cells from different cell layers within each root cross-section. The 'Path Intensity Profile' plugin in Icy was used to measure the maximum pixel intensity for each cell wall in the FY or BF channels. For background correction, random points along the root surface were selected to estimate the overall background signal for each image. The average background signal of each image was subtracted from the maximum pixel intensity of each cell wall. Finally, for each image, the fluorescence signal of the cell layer was determined as average signal intensity across all measured cells of the layer. Quantification was done using cross-sections of at least 8 individual roots in mock or ABA conditions and statistical differences were determined based on Wilcoxon rank-sum test with a Benjamini-Hochberg adjusted P-value threshold of 0.05 was used to indicate the statistical significance.

446 ***GC-MS***

447 For the profiling of suberin monomers, four-day-old seedlings of *C. arietinum* Anigiri and *V. sativa*
448 Prontivesa and two-day-old seedlings of *M. truncatula* A17, were transferred to magenta boxes
449 filled with sterile ½ MS medium supplemented with or without 2 µM ABA. A metal grid was placed
450 in the magenta boxes to ensure that only the root was in direct contact with the liquid medium.
451 The seedlings were maintained in the magenta boxes under long-day conditions (16 h light, 8 h
452 dark; 25°C; 70% humidity), under slow agitation (20 rpm) for 24 hours. Root samples (root tip to
453 the 50% region of the root) were collected for an average of 350, 210 and 50 mgs of fresh weight
454 (FW) tissue per biological replicate for *C. arietinum, V. sativa and M. truncatula*, respectively. Root
455 samples were immediately placed in hot isopropanol (70°C) for 30 minutes. The samples were
456 extracted using a Soxhlet apparatus for 8 hours, first with chloroform followed by methanol, to
457 eliminate all soluble lipids. Subsequently, extracted tissues were dried over silica gel in a
458 desiccator. Suberin monomers were released through transesterification with sulfuric acid in
459 methanol (5% v/v) at 85 °C for 3h. Dotriacontane (0.2 µg/µl) was added to each sample as an
460 internal standard. Sodium chloride (2.5% w/v) and methyl tert-butyl ether (MTBE) were added to
461 stop the transesterification reaction and to extract suberin monomers. The MTBE extract was
462 washed with sodium chloride (0.09% w/v) in Tris buffer (100mM) at pH8. The MTBE fraction was
463 then completely evaporated and subsequently derivatized with N,N-
464 bis(trimethylsilyl)trifluoroacetamide (BSTFA) and pyridine at 70°C for 40 minutes. Gas
465 chromatography (GC) equipped with a flame ionization detector (6890 N Network GC System,
466 Agilent Technologies) was used to separate and quantify the compounds. For compound
467 identification, gas chromatography coupled with a mass spectrometry selective detector (GC-
468 MS; 5977A MSD, Agilent Technologies) was utilized and fragmentation spectra were matched
469 against an internal library of known suberin monomers and the NIST database for identification.
470 Method was adapted from [68].

471

472 ***Transmission Electron Microscopy (TEM)***

473 Germinated seedlings of chickpea, *M. truncatula* and *V. sativa* were transferred for 3 days on
474 plates with either mock or 2 µM ABA treatment. After three days of treatment, 1 cm root pieces
475 were harvested in the 75% region of the individual roots. Root pieces were fixed in 2.5%
476 glutaraldehyde + 2% paraformaldehyde in phosphate buffer (PB 0.1 M) at 4°C for at least two
477 weeks. After incubation, samples were washed 6 times for 10 min in PB, incubated in 1% osmium
478 tetroxide dissolved in PB for 1 h, and washed again 3 times for 10 min using MilliQ water. Samples
479 were dehydrated using concentration gradient of acetone solutions (10% for 15 min, 30% for 15
480 min, 50% for 15 min, 70% for 15 min, 80% for 15 min, 90% for 15 min, 96% for 10 min, 100% for
481 15 min, 100% for 30 min). This was followed by infiltration with LR white in a concentration
482 gradient (1:2 LR white: EtOH for 1 h, 1:1 LR: EtOH for 1 h, 2:1 LR white: EtOH for 1 h, 100% LR
483 white for 2 h, 100% LR white overnight at room temp, 100% resin for 2 h) and polymerized for 24
484 h in an oven at 60-65°C. Polymerized samples were cross-sectioned to 50 nm thickness for *M.*
485 *truncatula* and chickpea, and *V. sativa* was sectioned to 70 nm thickness using a Leica
486 ultramicrotome UC7, before attaching to 100 mesh carbon grids. The grids were incubated for 10
487 min using 2% uranyl acetate followed by 5 washes with MilliQ water. Next, the grids were
488 incubated with lead citrate (EMS) for 10 min in a CO_2-free environment. The grids were washed
489 two times with 0.01 N CO_2-free water followed by 3 final washes with MilliQ water. Sample
490 preparation, processing and imaging were carried out by the Wageningen Electron Microscopy
491 Centre. A JEOL JEM1400 transmission electron microscope was used to image the samples.

492 ***Propidium iodide diffusion assay***

493 Four-day-old seedlings of *C. arietinum* Anigiri and *V. sativa* Prontivesa and two-day-old seedlings
494 of *M. truncatula* A17, were transferred to new ½ MS square plates supplemented with 2 µM ABA

or mock conditions. The seedlings were maintained in a D-root system[67] in growth chamber under long-day conditions (16 h light, 8 h dark; 25°C; 70% humidity). After 3 days, root segments up to the 75% region, including the root tip, were exposed to 30 µg/mL propidium iodide solution in the dark at 28 °C for 2 hours. Root segments were washed twice in MilliQ water and 0.5 cm segments from the 50% region of the root were excised and embedded in 4% (w/v) agarose for *C. arietinum* and *V. sativa* and in 3% (w/v) agarose for *M. truncatula*. Root cross-sections (250 µm thick) were obtained using the VT 1000 S vibratome (Leica). Optical laser scanning microscopy was performed on a Zeiss apotome microscope with the ×20 objective at 405 nm excitation and 600–650 nm detection. The quantification of the cell-layer PI intensity was done as described above.

RNAseq harvest, libraries, sequencing

Four-day-old seedlings of *C. arietinum* Anigiri were transferred to magenta boxes filled with sterile ½ MS medium supplemented with or without 2 µM ABA. Like the GC-MS experiments, chickpea seedlings were placed on top of a metal to ensure that only the root was in direct contact with the liquid medium. Seedlings were maintained in the magenta boxes under long-day conditions (16 h light, 8 h dark; 25°C; 70% humidity), under slow agitation (20 rpm) until the time of harvest. Lower 50% of the roots from the mock and ABA treatments were harvested at nine different timepoints: 15, 30 and 45 minutes, and 1 hour (h), 2h, 4h, 6h, 8h and 24h after ABA exposure. Three roots were sampled for each individual biological replicate. Samples were collected in 2-ml tubes containing ceramic beads and ground using a tissuelyser (Retsch MM300). The mRNA extraction and library preparation were performed according to a non-strand specific random primer-primed RNAseq library protocol[69]. The libraries were pair-end sequenced (150 bp) using NovaSeq X Plus.

RNAseq mapping, data analysis

Paired-end reads were quality trimmed using Trim Galore (version 0.6.6)[70] using default settings. After trimming, reads were pseudo-aligned to the CDC Frontier chickpea reference transcriptome (Phytozome, https://phytozome-next.jgi.doe.gov/) using Kallisto (version 0.46.2)[71] with the following parameters: -b 100. DEGs were identified using the R package limma according[72] to [28]. For every time point, we compared the ABA and mock treated samples using edgeR[73] and DEGs were determined as genes with an Benjamini-Hochberg adjusted P value < 0.05 and at least 2-fold changes between treatments (Supplementary Table 2). DEGs were clustered based on their logFC values across all time points using kmeans function from R (k=8) (Supplementary Table 2). Annotation of DEGs was based on annotation info for the CDC Frontier genome on Phytozome.

Promoter motif enrichment analysis

DNA motif enrichment analysis was performed as described[74], using the DNA motifs: GBOX (CACGTG), MYB41 (ACCTA), ATHB7 (ATNATTG), bHLH122 (CNACTTG), NF-YA (CCAAT), ANAC058 (CNTNNNNNNNANG), WRKY40 (TTGACT) and HAT5 (AATAATT) to screen the promoter regions (500 bps upstream the ATG) of DEGs identified in modules I, II, III, IV, V and VI. In summary, motifs were screened for enrichment using HOMER (homer.ucsd.edu/homer/motif/index.html) using the known function. For each DEG cluster, we generated 1000 sets of randomly selected genes that were of comparable number. Each set of promoters from each cluster were compared against the promoters of the respective 1,000 sets of random genes to calculate the P value significance of enrichment. P values were adjusted using the Bonferroni method, and a significance threshold of P < 0.01 was used to identify significantly enriched DNA motifs.

Phylogenetic tree construction

Phylogenetic trees were generated using the methods described in[28]. In summary, Full length amino acid sequences of chickpea ABA-upregulated MYBs (Supplementary Fig. 4a), WRKYs (Supplementary Fig. 4b) or the best five BLAST hits of lignin-regulating MYBs (Extended Data Fig.

543 5c-f) from Phytozome v 1.0 and all annotated Arabidopsis MYB or WRKY TFs from TAIR10 were
544 aligned using MAFFT (https://mafft.cbrc.jp/alignment/server/). The phylogenetic tree was
545 determined using the maximum likelihood method with 1000 bootstraps using iQ-TREE 3.1
546 (http://iqtree.cibiv.univie.ac.at/)[75].

547 ***Chickpea root protoplast isolation and scRNA-seq***

548 For the scRNA-seq analysis we used protoplasts from roots (3 cm above the root tip, which
549 corresponds to the middle-point of the root) of 3-day old chickpea seedlings grown in the
550 presence of 2 µM ABA for 24 h. Approximately 15 roots were collected, cut into 1-2 mm slices and
551 vacuum infiltrated for 15 minutes immersed in an enzyme solution consisting of 0.4 M D-Sorbitol,
552 20 mM KCl, 20 mM MES, 10 mM CaCl2, 0.1% (w/v) BSA, 1.5% (w/v) Cellulase R10 (Duchefa), 0.5%
553 (w/v) Macerozyme R10 (Duchefa), 5% (v/v) Viscozyme® L (Sigma) and 3.56 mM of 2-
554 Mercaptoethanol. Roots were kept in the enzyme solution for 2 h under 40 rpm, and the resulting
555 protoplast solution was filtered through a 40 µm mesh and centrifuged for 5 min at 200 x g at 4°C
556 in a swinging bucket centrifuge with the de-acceleration set to minimal. Protoplasts were
557 resuspended in 2 mL of resuspension solution (0.4 M D-Sorbitol, 20 mM KCl, 20 mM MES, 1 mM
558 CaCl2, 0.1% (w/v) BSA, 3.56 mM of 2-Mercaptoethanol). Chickpea root protoplasts were purified
559 using a three-phase density gradient using Optiprep™ (Stemcell™ Technologies). An Optiprep™
560 working solution (WS) was prepared by mixing 0.06 g of KCl into 10 mL of Optiprep™. The density
561 gradient was prepared in a 5 mL tube as follows: in the bottom layer, 2 mL of protoplast cell
562 suspension was gently mixed and homogenized with 500 µL of OptiPrep™ WS (final density: 1.064
563 g/mL). For the middle layer, 1 mL of a mixture of 2 mL of resuspension buffer with 400 of OptiPrep™
564 WS (final density: 1.053 g/mL) was gently pipetted at the top of the bottom layer. For the topmost
565 layer, 200 µL of the resuspension solution was carefully pipetted on top of the middle layer. The
566 prepared gradient was centrifuged at 200 x g at 4°C for 5 minutes using a swinging bucket
567 centrifuge. Following centrifugation, the protoplasts, concentrated in the topmost layer, were
568 carefully collected, centrifuged again for 5 min at 200 × g at 4°C and resuspended to a final
569 concentration of ~1,000 cells per µl in resuspension solution. The protoplast suspension was
570 loaded into microfluidic chips (10X Genomics) and subsequently processed using the 10x
571 Chromium Controller from 10x Genomics, Single-cell libraries were constructed using the Single
572 Cell 3' v3.1 Kit (10x Genomics) following manufacturer instructions. Sequencing was performed
573 using NovaSeq X Plus (PE150).

574 ***Single-cell transcriptome analysis***

575 Reads were mapped using cellranger (10X Genomics) to the CDC Frontier chickpea reference
576 genome (Phytozome, https://phytozome-next.jgi.doe.gov/) with appended chloroplast genome of
577 chickpea (NC_011163.1) and the mitochondrial genome of *M. truncatula* (NC_029641.1). For an
578 improved alignment, a modified version of the current Carietinum_492_v1.0 (Phytozome) was
579 used. Due to the 3' bias of sequencing reads generated by the 10X Single Cell 3' v3.1 library kit,
580 the 3' UTR regions of all genes in the chickpea genome were expanded by 500 bps using
581 BEDTools[76], as the Carietinum_492_v1.0 gene model lacks annotated 3' UTR regions. Before
582 analysis in Seurat[77], the fraction of background reads was removed using SoupX[78], cell doublets
583 were removed using scDblFinder, and low-quality cells were identified and removed based the
584 number of detected features (< 800 features) and mitochondrial and chloroplast gene counts (>
585 5% of mitochondrial and chloroplast counts), which resulted in the detection of 8,639 high-
586 quality cells. Uniform manifold approximation and projection (UMAP) were calculated using 50
587 principal component dimensions and cell-clusters were identified using the Seurat
588 'FindClusters' function with the resolution parameter set to 0.8. Markers for each UMAP cluster
589 were identified using the using the Seurat 'FindAllMarkers' and filtered for an average log2FC
590 greater or equal than 1, adjusted P values lower or equal 0.01, percentage of cells within the
591 cluster that expresses the gene greater than 20% and percentage difference to other clusters
592 greater than 20%. The identities of specific UMAP clusters were annotated by comparing whether

593 orthologues of marker genes were characterized as marker genes in the Arabidopsis scRNA-seq
594 root database (scPlantDB)[50] and those empirically determined from the Arabidopsis scRNA-seq
595 root atlas[51]. Additionally, the exodermis and endodermis cell clusters were identified based on
596 the expression of a manually curated list of suberin biosynthesis genes and Casparian strip
597 genes, respectively.

598 ***Lineage detection and pseudotime trajectory analysis***

599 Lineage detection and pseudotime trajectory was performed using the cell clusters representing
600 the outer ground tissue (outer cortex 1 & 2 and exodermis). The meristem_1 cluster was included
601 to anchor the cell lineage detection and pseudotime estimations. Lineage detection and
602 pseudotime trajectory were detected using the Slingshot R package[56] with the 'getLineages' and
603 'slingshot' functions, respectively.

604 ***Constructs for transactivation assays: promoters***

605 Promoter regions (~2 kb upstream of the start codon) were PCR-amplified from *Cicer arietinum*
606 Anigiri genomic DNA using the primers listed in Supplementary Table 4. The amplified fragments
607 were first cloned into the Gateway entry vector pDONR207 and then recombined into the
608 Gateway-compatible destination vector pGreenII 0800-LUC. In the case of *pCa_01018*, the
609 sequence was obtained pre-cloned in the pDONRZeo vector (GeneArt, Thermo Fisher Scientific)
610 and was recombined directly into the destination vector pGreenII 0800-LUC. The sequence used
611 is listed in Supplementary Table 4.

612 ***Constructs for transactivation assays: transcription factors***

613 Total RNA was extracted from roots of *C. arietinum* Anigiri grown in ½ MS agar plates in the
614 presence of ABA (2 µM) using the RNeasy Mini Kit (Qiagen), followed by DNase I treatment
615 (Thermo Fisher Scientific). cDNA synthesis was performed using the RevertAid RT Reverse
616 Transcription Kit (Thermo Fisher Scientific) with random hexamer primers. Coding sequences of
617 the TFs were amplified using primers listed in Supplementary Table 4, cloned into the Gateway
618 entry vector pDONR221, and subsequently recombined into the destination vector pH7WG2.

619 ***Transient Expression Assays in Nicotiana benthamiana agroinfiltrated leaves***

620 Competent *Agrobacterium tumefaciens* AGL-1 cells were transformed with the expression
621 constructs. Single colonies were cultured in 20 mL LB medium at 28°C for 2 days with shaking.
622 After reaching the desired OD600, the cultures were pelleted and resuspended to a final OD600
623 of 0.5 in half-strength MS medium (Duchefa Biochemie) supplemented with 10 mM MES hydrate
624 (Sigma-Aldrich), 20 g/L sucrose (Sigma-Aldrich), and 200 µM acetosyringone (Sigma-Aldrich),
625 adjusted to pH 5.6. The suspensions were incubated in darkness for 3–4 hours.

626 Agroinfiltration was performed on the abaxial side of 4-week-old *N. benthamiana* leaves using a
627 1 mL syringe. *Agrobacterium* strains carrying the promoter and transcription factor constructs
628 were mixed prior to infiltration. Plants were maintained under normal light conditions. One day
629 post-infiltration, the abaxial and adaxial sides of the infiltrated leaves were brushed with a
630 solution containing 0.01% (v/v) Tween-20 and either 20 mM ABA (in 70% ethanol) diluted in water
631 (final concentration of 75 µM) or a mock solution (equal volume of 70% ethanol in water). After
632 overnight incubation (16–18 h), leaf sections from the infiltrated regions were collected for
633 transactivation analysis. Firefly and Renilla luciferase activities were determined using the Dual-
634 Luciferase Reporter Assay System kit (Promega) and measured using the GloMax Navigator
635 microplate luminometer reader (Promega). Each transactivation assay was performed with 3 or
636 4 biological replicates at two independent experiments (Fig. 6e and Supplementary Fig. 11).

637

638 **Data availability**

All sequencing data and coding scripts will be openly released upon acceptance of the manuscript for publication.

Acknowledgements

We would like to thank Judith Boursin for pea seeds, Wouter Kohlen for *Medicago truncatula* seeds and extensive conversations, Tonni Andersen for *Lotus japonicus* seeds and support, and Laura Ragni and Bruno Guillotin for critical reading of the manuscript. We also thank Xiren Cao, Henri Essombé Kuoh and Menno Druif for technical assistance, and the WUR TEM facility for imaging.

Author contributions

KK: Conceptualization, Supervision, Project Administration, Funding Acquisition.
LJ, RK, SB, MR, JH, HC: Investigation.
RBF, PD: Resources.
LJ: Data Curation, Formal Analysis.
LJ, RK: Visualization.
LJ, KK: Original Draft.
All authors: Writing – Review & Editing.

Conflict of interest

No conflict of interest declared.

Funding statement

This work was supported by Netherlands Organization for Scientific Research (NWO) VIDI grant number VI.Vidi.193.104 to KK.

References

1. Barberon, M. *et al.* Adaptation of root function by nutrient-induced plasticity of endodermal differentiation. *Cell* **164**, 447–459 (2016).
2. Shukla, V. *et al.* Suberin plasticity to developmental and exogenous cues is regulated by a set of MYB transcription factors. *Proc. Natl. Acad. Sci. U. S. A.* **118**, e2101730118 (2021).
3. Cantó-Pastor, A. *et al.* A suberized exodermis is required for tomato drought tolerance. *Nat. Plants* **10**, 118–130 (2024).
4. Chen, X. *et al.* Four MYB transcription factors regulate suberization and non-localized lignification at the root endodermis in rice. *Plant Cell* (2024) doi:10.1093/plcell/koae278.
5. Shiono, K. *et al.* Abscisic acid is required for exodermal suberization to form a barrier to radial oxygen loss in the adventitious roots of rice (Oryza sativa). *New Phytol.* **233**, 655–669 (2022).
6. Su, Y. *et al.* The evolutionary innovation of root suberin lamellae contributed to the rise of seed plants. *Nat. Plants* **9**, 1968–1977 (2023).
7. Manzano, C. *et al.* Regulation and function of a polarly localized lignin barrier in the exodermis. *Nat. Plants* (2024) doi:10.1038/s41477-024-01864-z.
8. Alassimone, J., Naseer, S. & Geldner, N. A developmental framework for endodermal differentiation and polarity. *Proc. Natl. Acad. Sci. U. S. A.* **107**, 5214–5219 (2010).
9. Roppolo, D. *et al.* A novel protein family mediates Casparian strip formation in the endodermis. *Nature* **473**, 380–383 (2011).

10. Hosmani, P. S. *et al*. Dirigent domain-containing protein is part of the machinery required for formation of the lignin-based Casparian strip in the root. *Proc. Natl. Acad. Sci. U. S. A.* **110**, 14498–14503 (2013).
11. Lee, Y., Rubio, M. C., Alassimone, J. & Geldner, N. A mechanism for localized lignin deposition in the endodermis. *Cell* **153**, 402–412 (2013).
12. Doblas, V. G. *et al*. Root diffusion barrier control by a vasculature-derived peptide binding to the SGN3 receptor. *Science* **355**, 280–284 (2017).
13. Nakayama, T. *et al*. A peptide hormone required for Casparian strip diffusion barrier formation in Arabidopsis roots. *Science* **355**, 284–286 (2017).
14. Naseer, S. *et al*. Casparian strip diffusion barrier in Arabidopsis is made of a lignin polymer without suberin. *Proc. Natl. Acad. Sci. U. S. A.* **109**, 10101–10106 (2012).
15. Barberon, M. The endodermis as a checkpoint for nutrients. *New Phytol.* **213**, 1604–1610 (2017).
16. Geldner, N. The endodermis. *Annu. Rev. Plant Biol.* **64**, 531–558 (2013).
17. Andersen, T. G. & Drapek, C. The endodermis 1. in *Plant Roots* 90–103 (CRC Press, Boca Raton, 2024).
18. Liu, T. & Kreszies, T. The exodermis: A forgotten but promising apoplastic barrier. *J. Plant Physiol.* **290**, 154118 (2023).
19. Perumalla, C. J., Peterson, C. A. & Enstone, D. E. A survey of angiosperm species to detect hypodermal Casparian bands. I. Roots with a uniseriate hypodermis and epidermis. *Bot. J. Linn. Soc.* **103**, 93–112 (1990).
20. Peterson, C. A. & Perumalla, C. J. A survey of angiosperm species to detect hypodermal Casparian bands. II. Roots with a multiseriate hypodermis or epidermis. *Bot. J. Linn. Soc.* **103**, 113–125 (1990).
21. Perumalla, C. J., Chmielewski, J. G. & Peterson, C. A. A survey of angiosperm species to detect hypodermal Casparian bands. III. Rhizomes. *Bot. J. Linn. Soc.* **103**, 127–132 (1990).
22. Lashbrooke, J. *et al*. MYB107 and MYB9 homologs regulate suberin deposition in angiosperms. *Plant Cell* **28**, 2097–2116 (2016).
23. Baumgart, L. A. *et al*. Recruitment, rewiring and deep conservation in flowering plant gene regulation. *Nat. Plants* **11**, 1514–1527 (2025).
24. Dubos, C. *et al*. MYB transcription factors in Arabidopsis. *Trends Plant Sci.* **15**, 573–581 (2010).
25. Du, H. *et al*. The evolutionary history of R2R3-MYB proteins across 50 eukaryotes: New insights into subfamily classification and expansion. *Sci. Rep.* **5**, 11037 (2015).
26. Xu, H. *et al*. Transcriptional networks regulating suberin and lignin in endodermis link development and ABA response. *Plant Physiol.* **190**, 1165–1181 (2022).
27. Cohen, H., Fedyuk, V., Wang, C., Wu, S. & Aharoni, A. SUBERMAN regulates developmental suberization of the Arabidopsis root endodermis. *Plant J.* **102**, 431–447 (2020).
28. Jo, L. *et al*. Transcription factors SlMYB41, SlMYB92 and SlWRKY71 regulate gene expression in the tomato exodermis. *J. Exp. Bot.* (2025) doi:10.1093/jxb/eraf161.
29. Krishnamurthy, P., Vishal, B., Bhal, A. & Kumar, P. P. WRKY9 transcription factor regulates cytochrome P450 genes CYP94B3 and CYP86B1, leading to increased root suberin and salt tolerance in Arabidopsis. *Physiol. Plant.* **172**, 1673–1687 (2021).
30. Krishnamurthy, P. *et al*. Regulation of a cytochrome P450 gene CYP94B1 by WRKY33 transcription factor controls apoplastic barrier formation in roots to confer salt tolerance. *Plant Physiol.* **184**, 2199–2215 (2020).
31. Serra, O. & Geldner, N. The making of suberin. *New Phytol.* **235**, 848–866 (2022).
32. Artur, M. A. S. & Kajala, K. Convergent evolution of gene regulatory networks underlying plant adaptations to dry environments. *Plant Cell Environ.* **44**, 3211–3222 (2021).
33. Enstone, D. E., Peterson, C. A. & Ma, F. Root endodermis and exodermis: Structure, function, and responses to the environment. *J. Plant Growth Regul.* **21**, 335–351 (2002).

34. Taleisnik, E. Water retention capacity in root segments differing in the degree of exodermis development. *Ann. Bot.* **83**, 19–27 (1999).
35. Bani, M., Pérez-De-Luque, A., Rubiales, D. & Rispail, N. Physical and Chemical Barriers in Root Tissues Contribute to Quantitative Resistance to Fusarium oxysporum f. sp. pisi in Pea. *Front. Plant Sci.* **9**, 199 (2018).
36. Sharma, N. K. *et al.* MicroRNA397 regulates tolerance to drought and fungal infection by regulating lignin deposition in chickpea root. *Plant Cell Environ.* **46**, 3501–3517 (2023).
37. Schreiber, L., Hartmann, K., Skrabs, M. & Zeier, J. Apoplastic barriers in roots: chemical composition of endodermal and hypodermal cell walls. *J. Exp. Bot.* **50**, 1267–1280 (1999).
38. Brundrett, M. C., Kendrick, B. & Peterson, C. A. Efficient lipid staining in plant material with sudan red 7B or fluorol [correction of fluoral] yellow 088 in polyethylene glycol-glycerol. *Biotech. Histochem.* **66**, 111–116 (1991).
39. Lux, A., Morita, S., Abe, J. & Ito, K. An improved method for clearing and staining free-hand sections and whole-mount samples. *Ann. Bot.* **96**, 989–996 (2005).
40. Heslop-Harrison, Y., Heslop-Harrison, J. S. & Heslop-Harrison, J. Germination of Corylus Avellana l. (Hazel) pollen: Hydration and the function of the oncus. *Acta Bot. Neerl.* **35**, 265–284 (1986).
41. Dharmawardhana, D. P., Ellis, B. E. & Carlson, J. E. Characterization of vascular lignification in Arabidopsis thaliana. *Can. J. Bot.* **70**, 2238–2244 (1992).
42. Falk, H. & El-Hadidi, M. N. Der Feinbau der Suberinschichten verkorkter Zellwände. *Z. Naturforsch. B J. Chem. Sci.* **16**, 134–137 (1961).
43. Guiltinan, M. J., Marcotte, W. R., Jr & Quatrano, R. S. A plant leucine zipper protein that recognizes an abscisic acid response element. *Science* **250**, 267–271 (1990).
44. Choi, H., Hong, J., Ha, J., Kang, J. & Kim, S. Y. ABFs, a family of ABA-responsive element binding factors. *J. Biol. Chem.* **275**, 1723–1730 (2000).
45. Ng, L. M., Melcher, K., Teh, B. T. & Xu, H. E. Abscisic acid perception and signaling: structural mechanisms and applications. *Acta Pharmacol. Sin.* **35**, 567–584 (2014).
46. Zenker, S. *et al.* Many transcription factor families have evolutionarily conserved binding motifs in plants. *bioRxiv* (2024) doi:10.1101/2024.10.31.621407.
47. O'Malley, R. C. *et al.* Cistrome and epicistrome features shape the regulatory DNA landscape. *Cell* **166**, 1598 (2016).
48. Ortiz-García, P. *et al.* The indole-3-acetamide-induced Arabidopsis transcription factor MYB74 decreases plant growth and contributes to the control of osmotic stress responses. *Front. Plant Sci.* **13**, 928386 (2022).
49. Kosma, D. K. *et al.* AtMYB41 activates ectopic suberin synthesis and assembly in multiple plant species and cell types. *Plant J.* **80**, 216–229 (2014).
50. He, Z. *et al.* scPlantDB: a comprehensive database for exploring cell types and markers of plant cell atlases. *Nucleic Acids Res.* **52**, D1629–D1638 (2024).
51. Shahan, R. *et al.* A single-cell Arabidopsis root atlas reveals developmental trajectories in wild-type and cell identity mutants. *Dev. Cell* **57**, 543-560.e9 (2022).
52. Liberman, L. M., Sparks, E. E., Moreno-Risueno, M. A., Petricka, J. J. & Benfey, P. N. MYB36 regulates the transition from proliferation to differentiation in the Arabidopsis root. *Proc. Natl. Acad. Sci. U. S. A.* **112**, 12099–12104 (2015).
53. Kamiya, T. *et al.* The MYB36 transcription factor orchestrates Casparian strip formation. *Proc. Natl. Acad. Sci. U. S. A.* **112**, 10533–10538 (2015).
54. Xie, M. *et al.* Regulation of lignin biosynthesis and its role in growth-defense tradeoffs. *Front. Plant Sci.* **9**, 1427 (2018).
55. Zhou, J., Lee, C., Zhong, R. & Ye, Z.-H. MYB58 and MYB63 are transcriptional activators of the lignin biosynthetic pathway during secondary cell wall formation in Arabidopsis. *Plant Cell* **21**, 248–266 (2009).
56. Street, K. *et al.* Slingshot: cell lineage and pseudotime inference for single-cell transcriptomics. *BMC Genomics* **19**, (2018).

57. Bakshi, M. & Oelmüller, R. WRKY transcription factors: Jack of many trades in plants. *Plant Signal. Behav.* **9**, e27700 (2014).
58. Kajala, K. *et al.* Innovation, conservation, and repurposing of gene function in root cell type development. *Cell* **184**, 3333-3348.e19 (2021).
59. Lu, H.-P. *et al.* An ABA-serotonin module regulates root suberization and salinity tolerance. *New Phytol.* **236**, 958–973 (2022).
60. Zhou, X., Lei, Z. & An, P. Post-translational modification of WRKY transcription factors. *Plants* **13**, 2040 (2024).
61. Adachi, H. *et al.* WRKY transcription factors phosphorylated by MAPK regulate a plant immune NADPH oxidase in Nicotiana benthamiana. *Plant Cell* **27**, 2645–2663 (2015).
62. Yao, Q., Gao, J., Bollinger, C., Thelen, J. J. & Xu, D. Predicting and analyzing protein phosphorylation sites in plants using musite. *Front. Plant Sci.* **3**, 186 (2012).
63. Hou, Y. *et al.* SAPK10-mediated phosphorylation on WRKY72 releases its suppression on jasmonic acid biosynthesis and bacterial blight resistance. *iScience* **16**, 499–510 (2019).
64. Park, S.-Y. *et al.* Abscisic acid inhibits type 2C protein phosphatases via the PYR/PYL family of START proteins. *Science* **324**, 1068–1071 (2009).
65. Zhu, M. *et al.* Single-cell transcriptomics reveal how root tissues adapt to soil stress. *Nature* (2025) doi:10.1038/s41586-025-08941-z.
66. Kreplak, J. *et al.* A reference genome for pea provides insight into legume genome evolution. *Nat. Genet.* **51**, 1411–1422 (2019).
67. Silva-Navas, J. *et al.* D-Root: a system for cultivating plants with the roots in darkness or under different light conditions. *Plant J.* **84**, 244–255 (2015).
68. Delude, C., Vishwanath, S. J., Rowland, O. & Domergue, F. Root aliphatic suberin analysis using non-extraction or solvent-extraction methods. *Bio Protoc.* **7**, e2331 (2017).
69. Townsley, B. T., Covington, M. F., Ichihashi, Y., Zumstein, K. & Sinha, N. R. BrAD-seq: Breath Adapter Directional sequencing: a streamlined, ultra-simple and fast library preparation protocol for strand specific mRNA library construction. *Front. Plant Sci.* **6**, 366 (2015).
70. Krueger, F. A wrapper tool around Cutadapt and FastQC to consistently apply quality and adapter trimming to FastQ files 516. **517**, (2015).
71. Bray, N. L., Pimentel, H., Melsted, P. & Pachter, L. Near-optimal probabilistic RNA-seq quantification. *Nat. Biotechnol.* **34**, 525–527 (2016).
72. Ritchie, M. E. *et al.* limma powers differential expression analyses for RNA-sequencing and microarray studies. *Nucleic Acids Res.* **43**, e47 (2015).
73. Robinson, M. D., McCarthy, D. J. & Smyth, G. K. edgeR: a Bioconductor package for differential expression analysis of digital gene expression data. *Bioinformatics* **26**, 139–140 (2010).
74. Jo, L. *et al.* Combinatorial interactions of the LEC1 transcription factor specify diverse developmental programs during soybean seed development. *Proc. Natl. Acad. Sci. U. S. A.* **117**, 1223–1232 (2020).
75. Wong, T. *et al.* IQ-TREE 3: Phylogenomic inference software using complex evolutionary models. *EcoEvoRxiv* (2025) doi:10.32942/x2p62n.
76. Quinlan, A. R. & Hall, I. M. BEDTools: a flexible suite of utilities for comparing genomic features. *Bioinformatics* **26**, 841–842 (2010).
77. Hao, Y. *et al.* Dictionary learning for integrative, multimodal and scalable single-cell analysis. *Nat. Biotechnol.* **42**, 293–304 (2024).
78. Young, M. D. & Behjati, S. SoupX removes ambient RNA contamination from droplet-based single-cell RNA sequencing data. *Gigascience* **9**, (2020).
79. Cannon, S. B. *et al.* Polyploidy did not predate the evolution of nodulation in all legumes. *PLoS One* **5**, e11630 (2010).
80. Ellis, T. H. N. *et al.* The taxonomic status of genera within the Fabeae (Vicieae), with a special focus on Pisum. *Diversity (Basel)* **16**, 365 (2024).

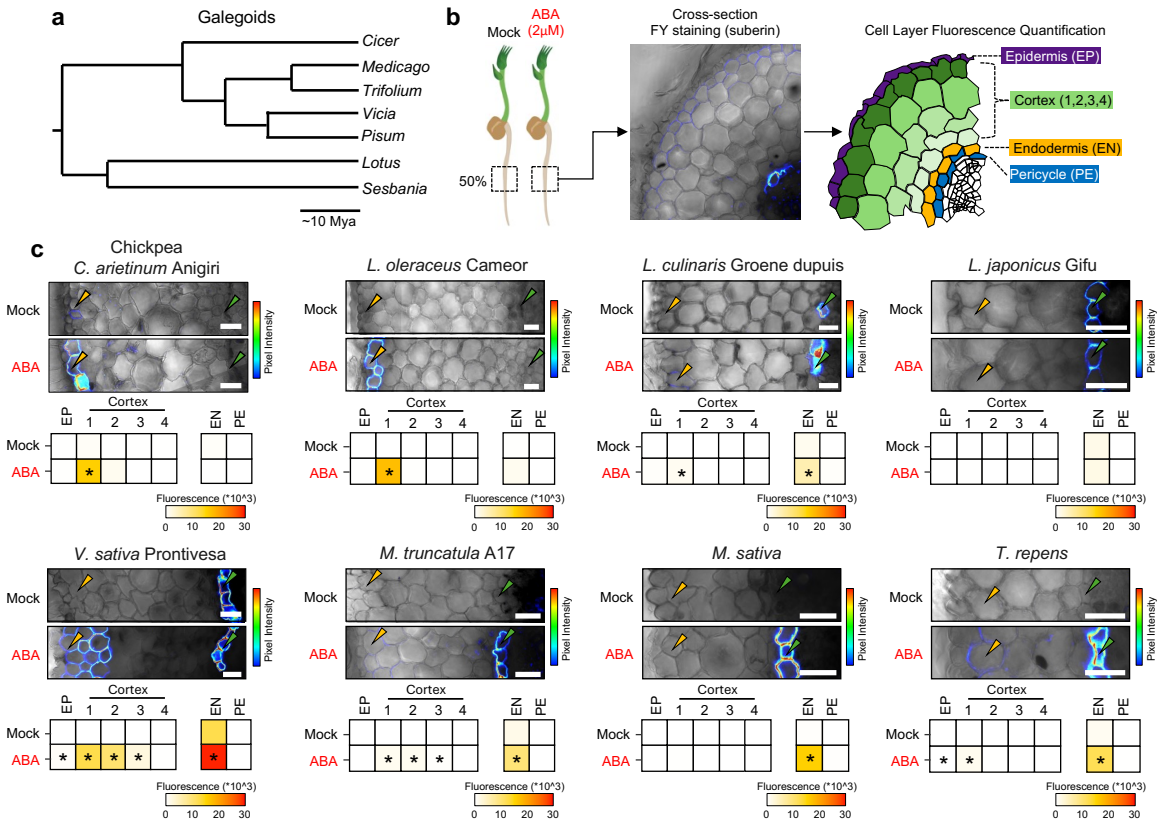

Figure 1. Galegoid legumes deposit suberin to the cell walls of different root cell types in response to ABA.

a, Representative phylogenetic tree of the galegoid legume clade. The tree was adapted from[79]. *Lens culinaris* is nested in the genus *Vicia*[80]. **b,** Graphical representation of the survey for observing cell-type suberization in legume roots treated with mock or ABA (2 μM) for 3 days. The middle point of the root (50%) was cross-sectioned, stained with FY and counter-stained with aniline blue. Finally, the fluorescence levels of cell walls of individual cell layers of the root epidermis (EP), the four outermost cortex layers (C1 to C4) out of the up to 12 cortex layers (depending on the species), the endodermis (EN) and the pericycle (PE) were quantified. **c,** Quantification summary of FY intensity across multiple cell layers of legume roots in response to ABA. For each species, the top images show representative confocal images of cross-section of roots treated with mock or ABA, with the FY signal overlaid on top of bright field images (scale = 25 μm). The yellow and green arrow depicts the position of the outermost layer of the cortex (C1) and endodermis, respectively. On the bottom, the heatmaps show the average pixel intensity of the FY signal in different layers of the root cross section. Asterisks indicate significance based on Wilcoxon rank-sum test with a Benjamini-Hochberg adjusted P-value. Threshold of 0.05 was used to indicate the statistical significance ($n \geq 8$).

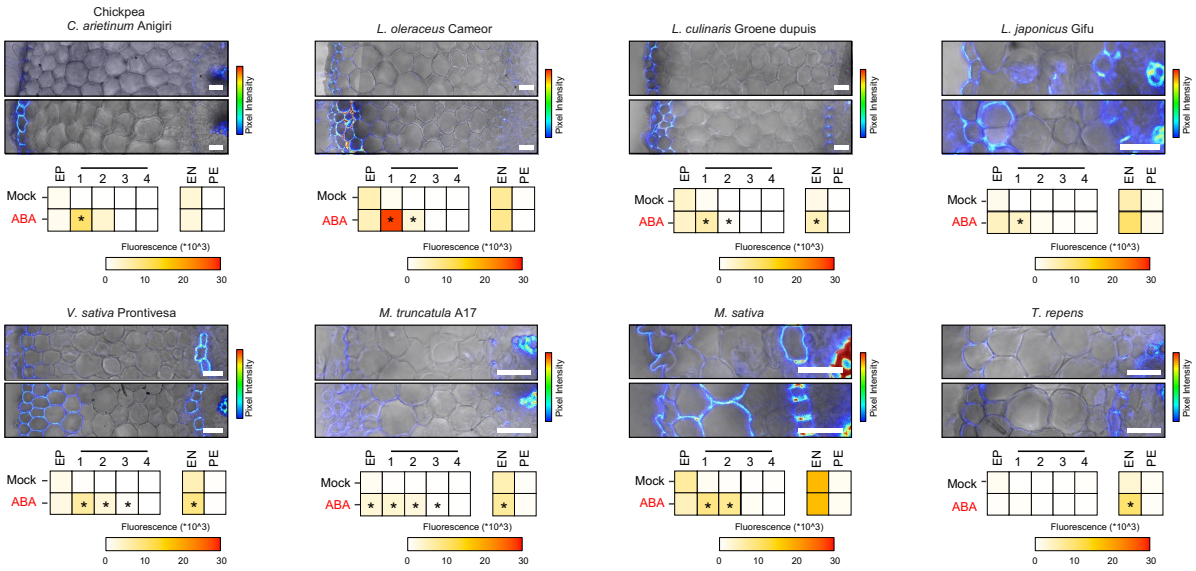

Extended Data Figure 1. Quantification summary of Basic Fuchsin (BF) dye intensity across multiple cell layers of legume roots in response to ABA.

For each species, the top images show representative confocal images of cross-section of roots treated with mock or ABA (2 μM) for 3 days, with the signal of BF overlaid on top of bright field images (scale = 25 μm). The bottom heatmap shows the average pixel intensity of the BF signal in different layers of the root cross section. Asterisks indicate significance based on Wilcoxon rank-sum test with a Benjamini-Hochberg adjusted P-value threshold of 0.05 was used to indicate the statistical significance ($n \geq 8$).

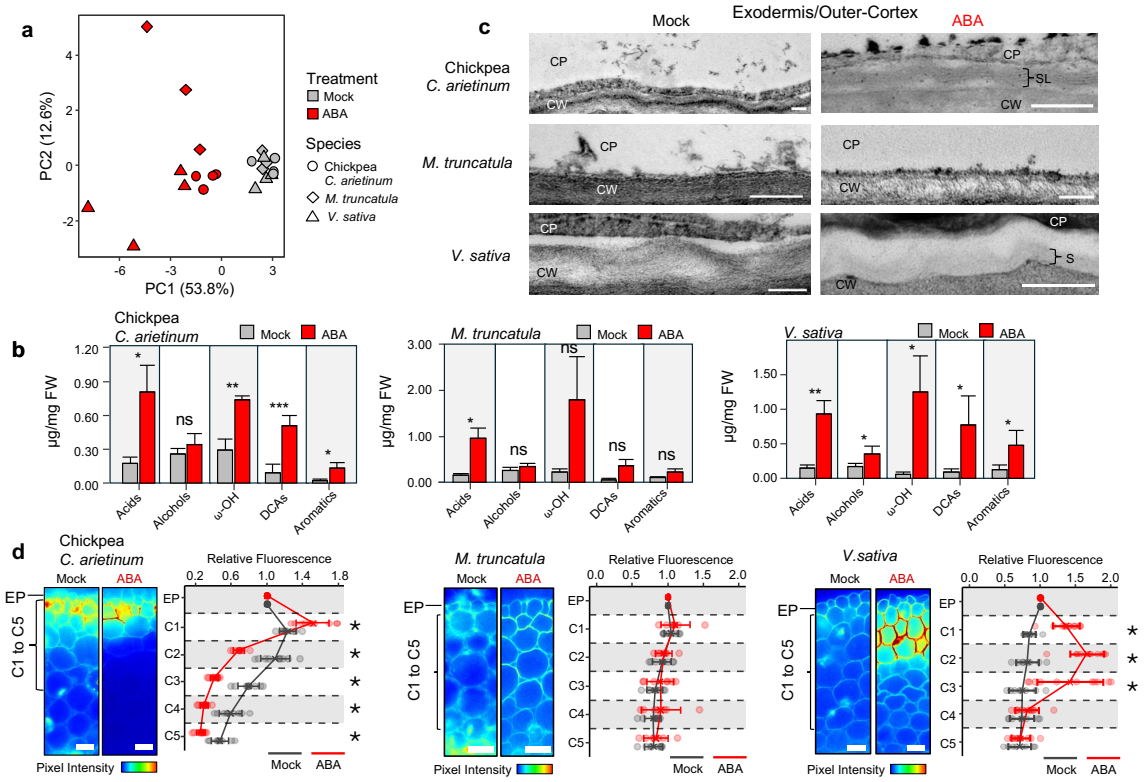

Figure 2. Biochemical, structural and functional evaluation of ABA-induced cell wall modifications show that chickpea forms an exodermis with a suberin lamella and an apoplastic diffusion barrier.

a, Principal Component Analysis (PCA) of suberin monomer abundances in roots of chickpea, *M. truncatula* and *V. sativa* treated with mock or 2 µM ABA for 24 hours. **b,** Abundance of major classes of suberin monomers in roots treated with mock (grey) or 2 µM ABA (red) for 24 hours. Asterisks indicate significance based on Student's t-test with a P-value threshold of 0.05 (n = 4). **c,** Outermost cortex cell wall shown in transmission electron microscopy (TEM) images of root cross-sections at the 50% region of Chickpea, *M. truncatula* and *V. sativa* roots treated with mock or 2 µM ABA for 3 days. The cell wall (CW) depicted in the images refers to the cell wall between two adjacent cells of the exodermis (in chickpea) or in the outermost cortex layer (in *M. truncatula* and *V. sativa*). Scale bar, 200 nm. SL: suberin lamellae; S: suberin; CW: cell wall; CP: cytoplasm. **d,** Propidium Iodide (PI) diffusion assay of chickpea, *M. truncatula* and *V. sativa* roots after treatment with mock (black) or 2 µM ABA (red) for 3 days. For each species, the left image shows a representative image of laser scanning confocal microscopy for PI in root cross-sections, with the PI signal indicating diffusion across epidermal and cortex cells. Scale bar, 25 µm. On the right, line plots show the relative pixel intensity of the PI dye cell wall in different layers of the root cortex (C1 to C5) relative to the intensity of the signal detected in the epidermis (EP). Asterisks indicate significance based on Wilcoxon rank-sum test with statistical significance of $P < 0.05$ ($n \geq 6$).

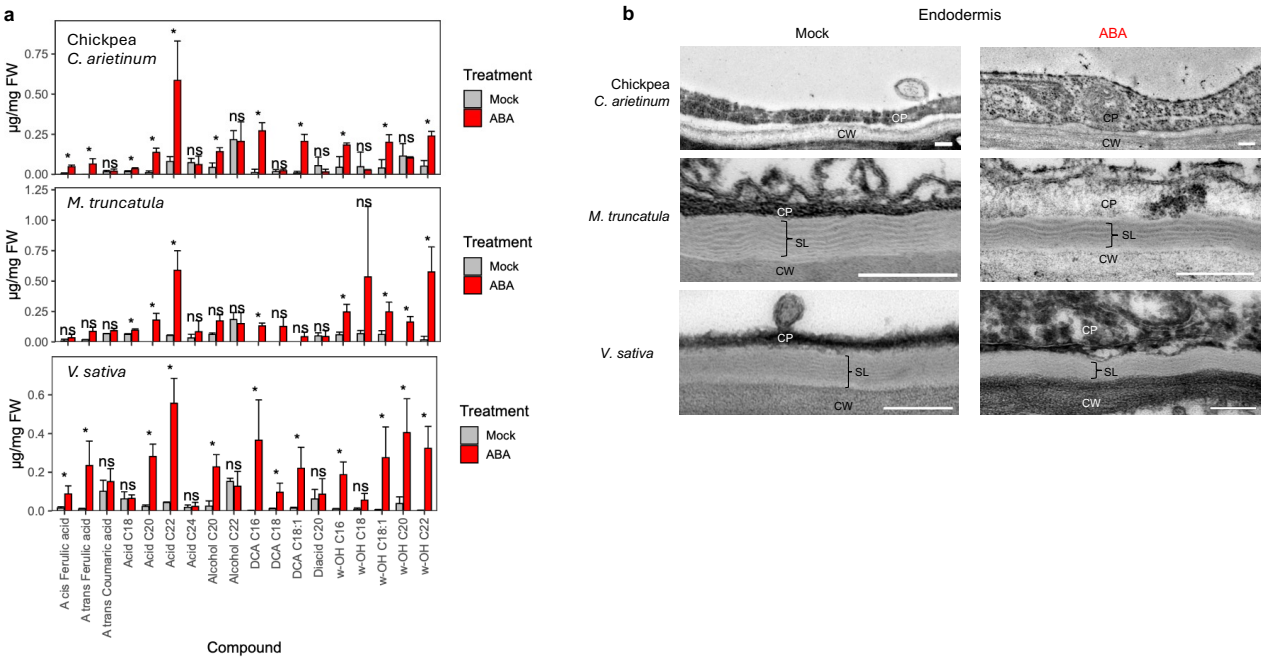

Extended Data Figure 2. Biochemical and structural evaluation of ABA-induced cell wall modifications.

a, Bar charts showing the abundance (µg/mg of fresh-weight (FW)) of individual suberin monomers in roots treated with mock (grey) or 2 µM ABA (red) for 24 hours. Asterisks indicate significance based on Student's t-test with a P-value threshold of 0.05 (n = 4). **b,** Endodermis cell wall shown in TEM images of cross-sections at the 75% root region of Chickpea, *M. truncatula* and *V. sativa* treated with mock or 2 µM ABA for 3 days. The cell wall depicted in the images refers to the cell-wall between two adjacent endodermal cells. Scale bar, 200 nm. SL: suberin lamellae; CW: cell wall; CP: cytoplasm.

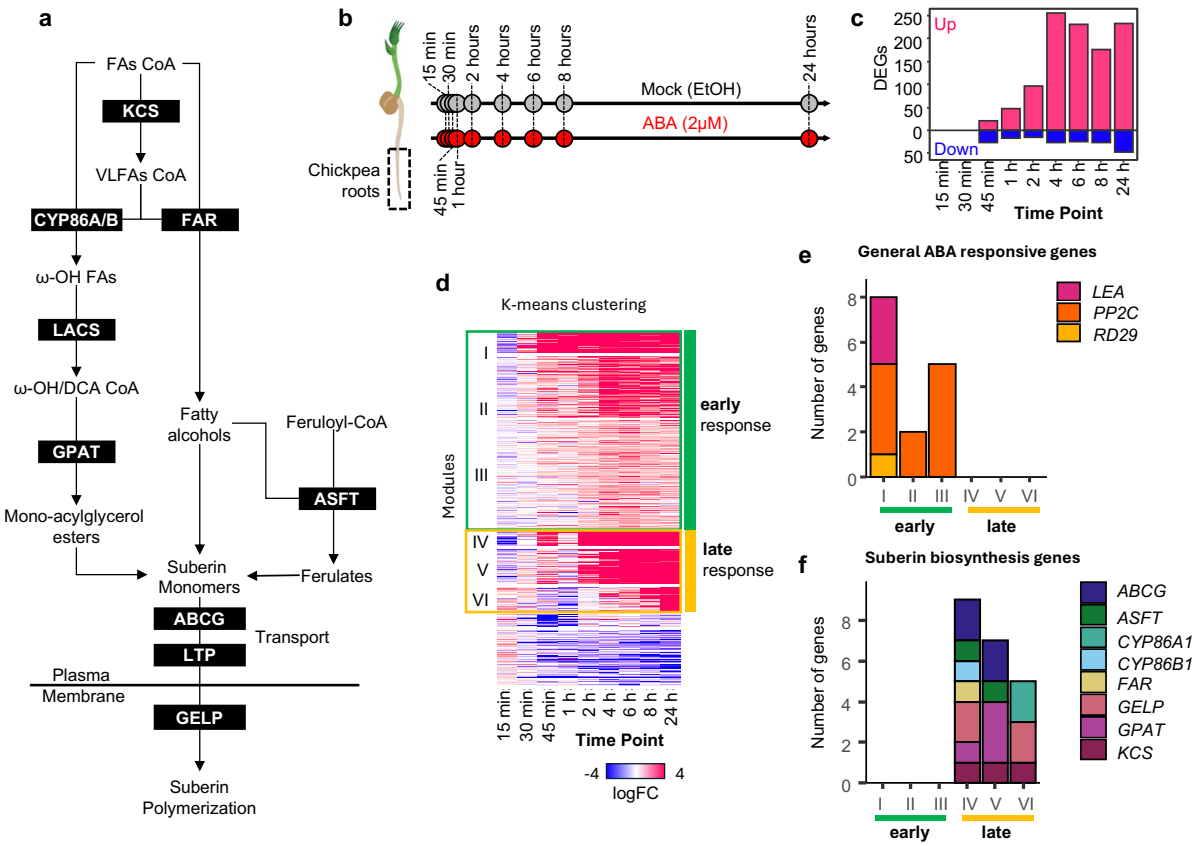

Figure 3. ABA induces temporally separated general ABA response and suberin biosynthesis programs in chickpea roots.

a, Simplified schematic diagram of suberin biosynthesis, transport and polymerization adapted from[3]. Black boxes indicate enzymes or transport proteins involved in each step of the pathway. FAs: fatty-acids; VLFA: very-long fatty-acids; KCS: 3-ketoacyl-CoA synthase; FAR: Fatty acyl-CoA reductase; CYP86A/B: cytochrome P450, family 86, subfamily A or B; LACS: long-chain acyl-coenzyme A synthetase; GPAT: glycerol-3-phosphate acyltransferase; ASFT: Aliphatic suberin feruloyl-transferase; ABCG: ABC transporter G; LTP: lipid transfer protein; GELP: GDSL esterase/lipases. **b,** Schematic representations of time points (15, 30 and 45 minutes (min) and 1, 2, 4, 6, 8 and 24 hours (h) used to profile the transcriptome changes of roots (lower half of the root) from 3-day old chickpea treated with mock (grey) and 2 μM ABA (red). **c**, Number of differentially expressed genes (DEGs) at each time point for ABA-treated roots compared with mock. DEGs were determined as genes with an Benjamini-Hochberg adjusted P value ≤ 0.05 and log2FC ≥ 1 (upregulated, pink) or log2FC ≤ -1 (downregulated, blue). The full lists of DEGs are given in Supplementary Table 2. **d**, Temporal modules detection using K-means clustering of DEGs (k = 8). The heatmap shows logFC values of each gene at each timepoint. For further analysis, we focused on six modules that had the highest upregulation in response to ABA (Modules I, II, III, IV, V and VI). These modules were grouped into two groups: early (I, II and III) and late (IV, V and VI) response to ABA based on their temporal profile (Extended Data Fig. 3a). The list of genes in temporal modules is given in Supplementary Table 2. **e**, Number of chickpea genes related to the canonical ABA response identified in modules I-VI. *LEA*: *LATE EMBRYOGENESIS ABUNDANT*; *PP2C*: *PROTEIN PHOSPHATASE 2C*; *RDB29B*: *RESPONSIVE TO DESICCATION 29B*. **g**, Number of chickpea genes related to suberin biosynthesis, transport and polymerization (listed in **a**) in modules I-VI.

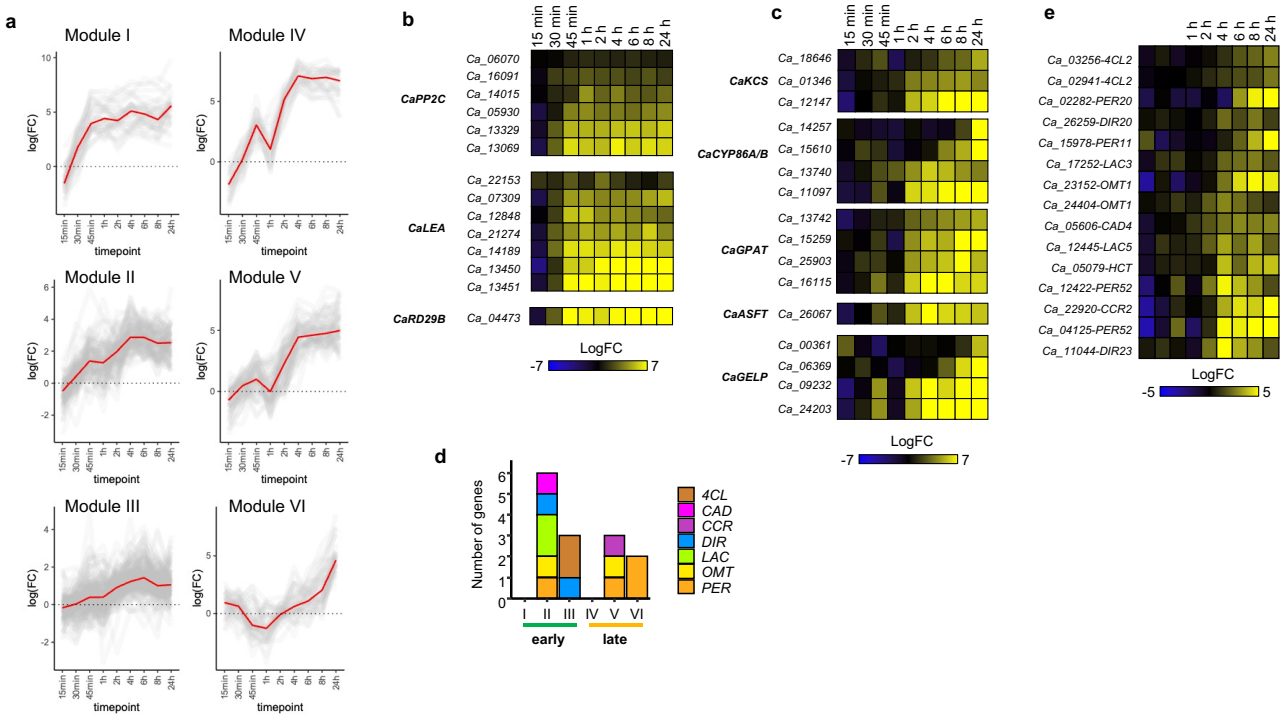

Extended Data Figure 3. Expression profiles of putative ABA response genes, suberin biosynthesis genes and lignin biosynthesis genes.

a, Lineplot showing the log of fold change (FC) of all genes (grey) in modules I-IV. Red lines depict median logFCs in each module. **b**, Heatmap showing the log(FC) of putative ABA response genes identified as DEGs. **c**, Heatmap showing the log(FC) of suberin biosynthesis genes identified as DEGs. **d**, Number of chickpea genes related to lignin biosynthesis identified in modules I-VI. **e**, Heatmap showing the log(FC) of lignin biosynthesis genes identified as DEGs.

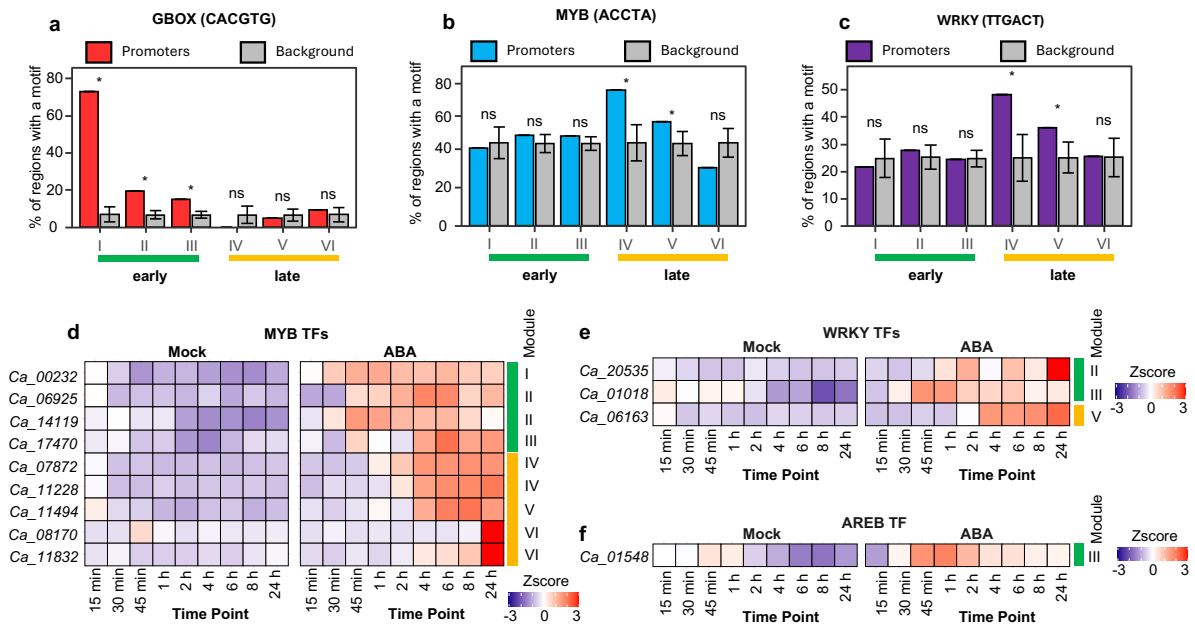

Figure 4. Putative mechanisms of the temporal distinction between ABA response and suberin biosynthesis program in chickpea roots.

a, GBOX (CACGTG), **b,** MYB41 (ACCTA) and **c**, WRKY40 (TTGACT) motifs enrichment in the module I-VI promoters (500 base pairs (bps) upstream the start codon (ATG) of each gene). Bar graphs show the percentage of promoters of DEGs (colored) and 1000 sets of promoters of randomly selected genes with equivalent number to the compared DEG list (grey) containing the indicated DNA motifs. A Bonferroni-adjusted P-value threshold of 0.01 was used to indicate the statistical significance (*) of enrichment, while ns indicates no significance. Expression of **d,** *MYB*, **e**, *WRKY* and **f**, *AREB* DEGs. Heatmaps show relative mRNA levels of chickpea treated with mock and 2 µM ABA for 15, 30 and 45 minutes (min) and 1, 2, 4, 6, 8 and 24 hours (h). The temporal module corresponding to each gene is specified.

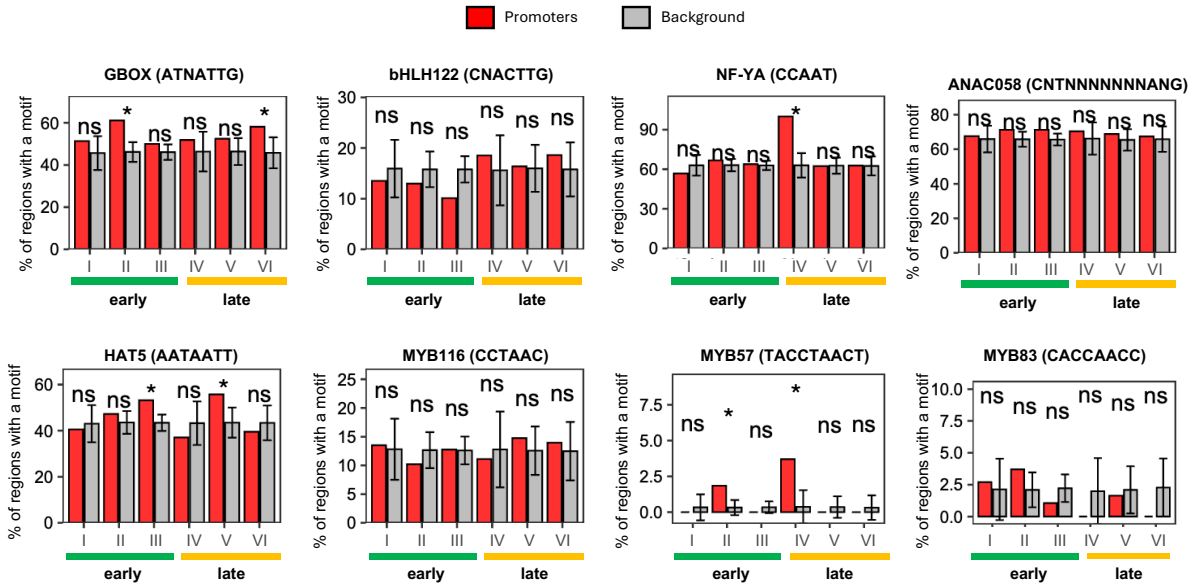

Extended Data Figure 4. DNA motif enrichment in the module I-VI gene promoters.

The selection of the above motifs was based on existing transcription factor families identified as DEGs (Supplementary Table 2). Bar graphs show the percentage of promoters of DEGs (red) and 1000 sets of promoters of randomly selected genes with equivalent number to the compared DEGs list (grey) containing the indicated DNA motifs. A Bonferroni-adjusted P-value threshold of 0.01 was used to indicate the statistical significance (*) of enrichment, while ns indicates no significance.

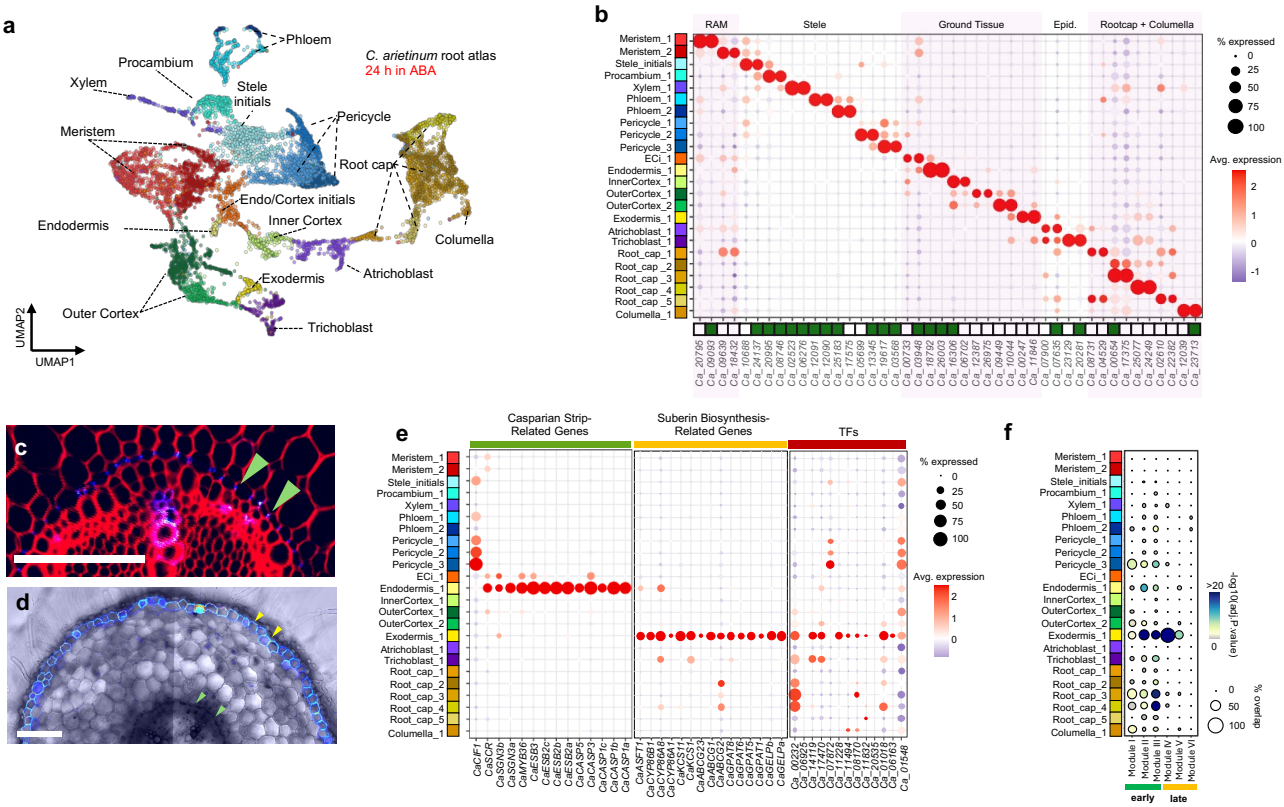

Figure 5. Single cell atlas of the chickpea root treated with ABA.

a, Twenty-two single-cell clusters of the chickpea root treated with 2 µM ABA for 24h, here shown as an integrated UMAP with their respective annotated cell identities. The list of marker genes for each single-cell cluster is presented in Supplementary Table 3. **b**, Expression of the top 2 marker genes for each cluster. Dot size indicates the percentage of cells in the cluster that expresses the specific gene (% expressed). Dot colors represent the average scaled expression of genes in the clusters (Avg. expression). The top 2 markers were identified by looking at the genes with the lowest adjusted P-values and the greatest percentage differences with other clusters. In the bottom of the dotplot, a green filled square indicates if the marker gene has an orthologue annotated as a marker gene in equivalent cell type in the Arabidopsis root scPlantdb[50]. We manually curated the datasets in the scPlantdb by only keeping datasets in which *AtMYB36* was annotated as a marker for the endodermal cell cluster. **c**, Root cross section of chickpea roots grown in mock conditions stained with basic-fuchsin (BF) and calcofluor white. BF (blue) staining depicts the lignification of the Casparian strip in the root endodermis (green arrow). Calcofluor white (red) stains general cell walls. **d**, Cross sections of chickpea roots grown with 2 µM ABA stained with FY and counter-stained with aniline blue, showing that the suberin accumulation only occurs in the root exodermis (yellow arrow). Scale: 100 µm. **e**, Dotplot showing the spatial expression in the single-cell data of Casparian strip related genes (left), suberin biosynthesis related genes (middle) and *MYB, WRKY* and *AREB* TFs identified as upregulated DEGs in the time course bulk RNA-seq experiment. The list of gene ids for Casparian strip and suberin biosynthesis are listed in the Supplementary Table 3. **f**, Statistical significance of the overlap between genes in the bulk RNA-seq temporal module (Fig. 3d) and gene markers of each single-cell cluster. In the dotplot heatmap, the size of the bubble depicts the percentage of genes in the temporal modules that are identified as gene markers for the single-cell clusters and the color represents the statistical significance of the overlap (hypergeometric distribution).

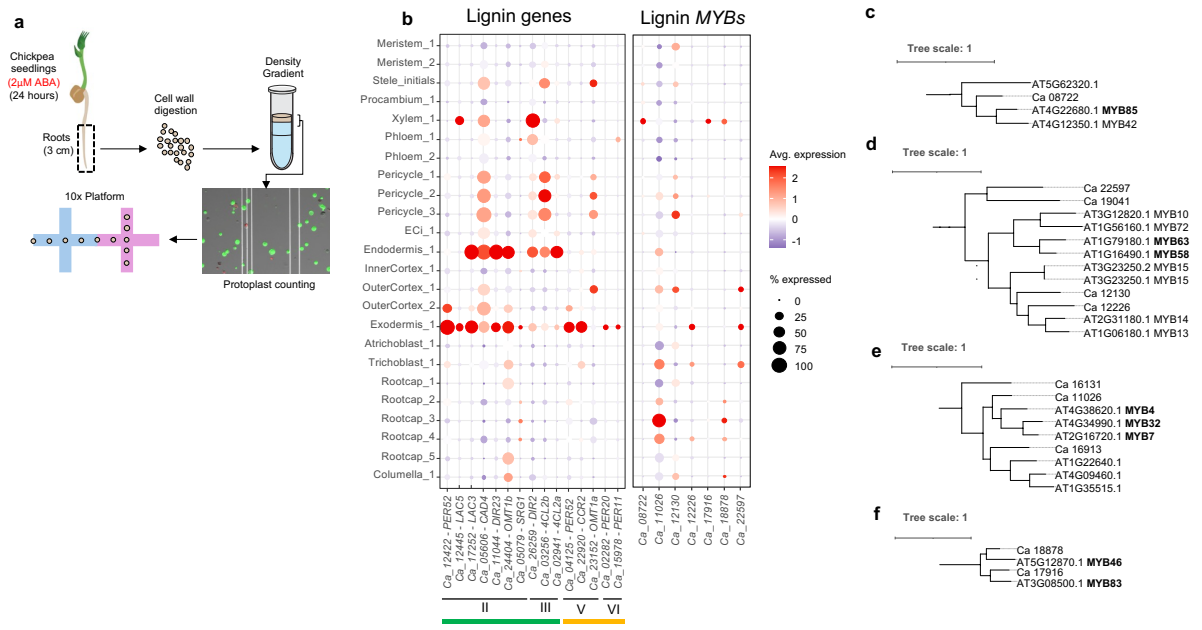

Extended data Figure 5. Expression of ABA-induced lignin biosynthesis and putative lignin regulators in the chickpea single cell atlas.

a, Overview of the scRNA-seq experiment in chickpea roots. 3-day-old chickpea seedlings were transferred to ½ MS medium plates containing 2 μM ABA. After 24 hours, protoplasts were released from roots (3 cm above the root tip) and loaded into the 10X Genomics Chromium chip for making the single-cell transcriptome libraries. **b**, Dotplot showing the spatial expression of ABA-induced lignin biosynthesis genes (left) and homologs of known lignin-regulating *MYB* TFs (right) in the single-cell dataset. **c, d, e, f,** Phylogenetic analysis identifying the relationships of closest chickpea homologs with the known Arabidopsis regulators of lignin biosynthesis: inducers AtMYB85 (**c**), AtMYB63 and AtMYB58 (**d**), inhibitors AtMYB4, AtMYB7 and AtMYB32 (**e**) and master regulators of secondary cell wall biosynthesis AtMYB46 and AtMYB83 (**f**).

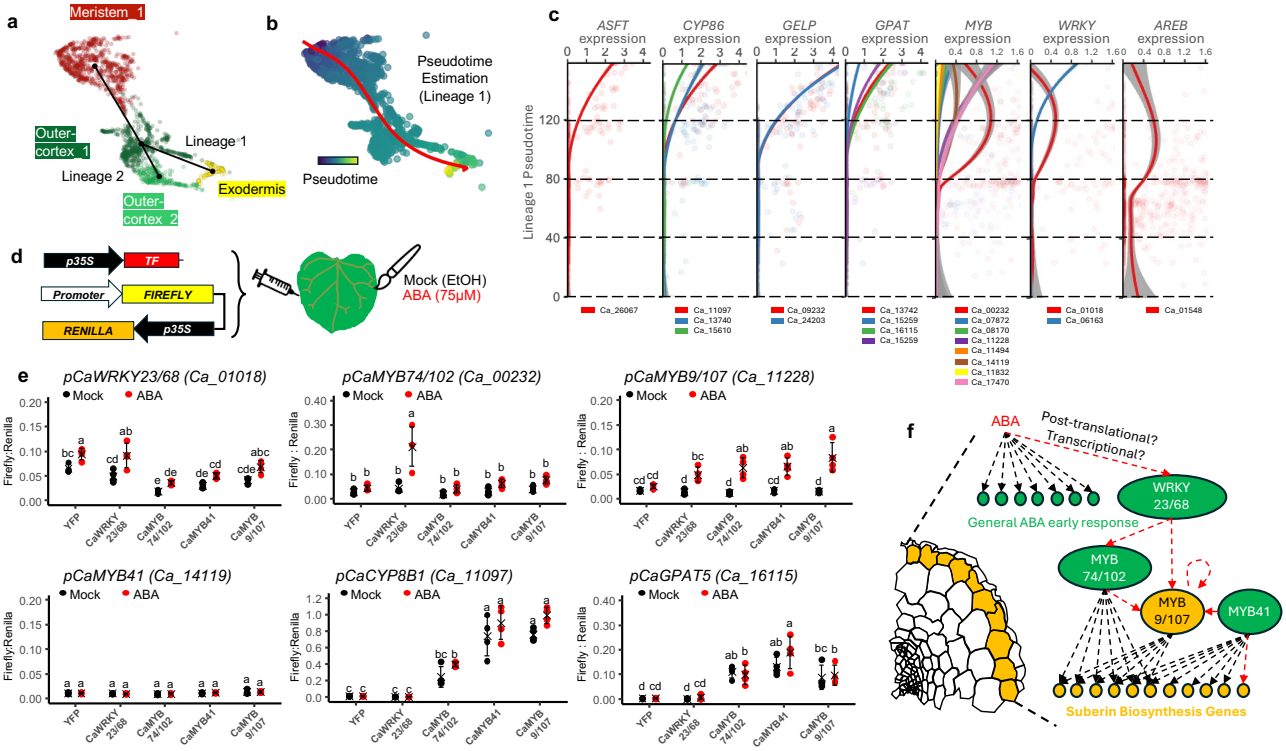

Figure 6. Pseudotime estimation recapitulates the temporal dynamics of *MYB* and *WRKY* leading the differentiation of exodermis in chickpea roots.

a, Cell lineage detection using the Slingshot package[56] revealed two lineages in the outer ground tissue (outer cortex and exodermis). The Meristem_1 cluster was included to help anchor the cell lineage detection and pseudotime estimations. Lineage 1 consists of clusters Meristem_1, Outercortex_1 and Exodermis_1, while Lineage 2 consists of Meristem_1, Outercortex_1 and Outercortex_2. **b**, Pseudotime trajectory through cell populations of Lineage 1. **c**, Scaled expression profiles of suberin biosynthesis genes (*ASFT*, *CYP86A/Bs*, *GELPs*, *GPATs*), *MYBs*, *WRKYs* and *AREB* along the Lineage 1 pseudotime trajectory. **d**, Schematic diagram of transactivation assays in *Nicotiana benthamiana* leaves. *N. benthamiana* leaves were co-infiltrated with i) the reporter vector carrying the firefly luciferase under the control of the promoter of interest and the transformation expression control (*p35S:RENILLA*) and (ii) vectors overexpressing each candidate TF (*p35S:TF*). A vector overexpressing the YFP protein was used as a transactivation negative control. After 24 hours, infiltrated leaves were brushed with a solution containing either 75 μM ABA or a mock solution. After overnight incubation (16–18 h), leaf sections were collected for transactivation analysis. **e**, The firefly to renilla luciferase activity ratios of each promoter in response to the TF (x-axis) in mock (black) and ABA (red) conditions are presented. The black mark indicates the mean and error bars represent the standard deviation ($n = 4$). Different letters indicate statistically significant differences (one-way ANOVA followed by a post-hoc Tukey test, $P \leq 0.05$). All transactivation assays were carried out twice (Supplementary Fig. 11). **f**, The working model for the suberization of chickpea exodermis. CaWRKY23/68 is induced and activated by ABA, and it induces two downstream *MYBs*, *CaMYB74/102* and *CaMYB9/107*. These and *CaMYB41* drive expression of suberin biosynthesis genes. Green color indicates expression in early modules, yellow in late modules. Red arrows indicate a positive interaction in presence of ABA, and black arrows indicate positive interaction regardless of ABA treatment.

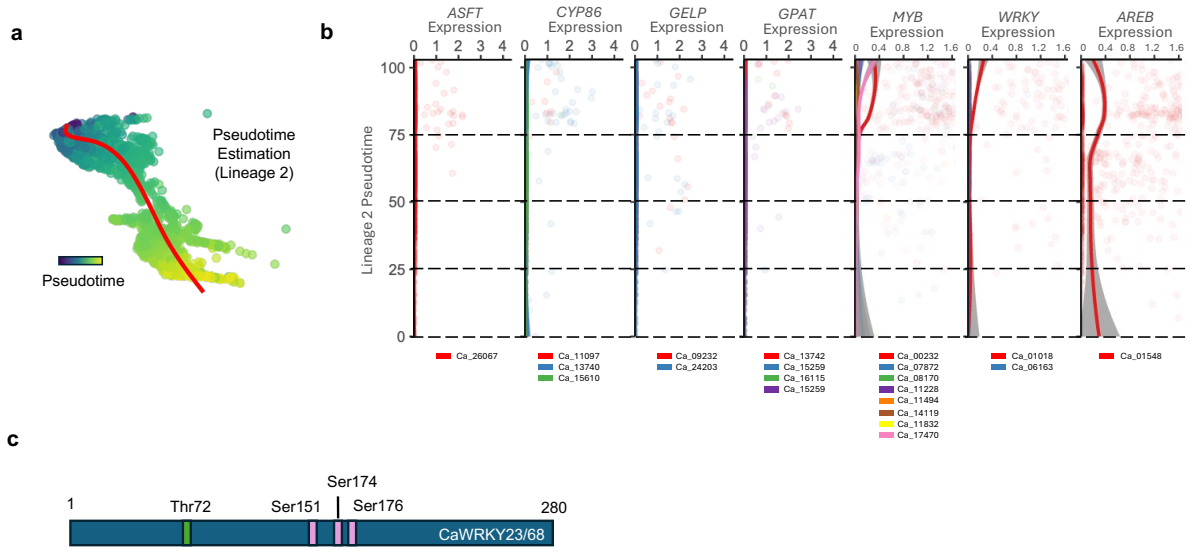

Extended Data Figure 6. Pseudotime trajectory of Lineage 2 does not involve suberin genes.

a, Pseudotime trajectory through cell populations of Lineage 2 (Meristem_1, Outercortex_1 and Outercortex_2). **b**, Scaled expression profiles of suberin biosynthesis genes (*ASFT*, *CYP86A/Bs*, *GELPs*, *GPATs*), *MYBs*, *WRKYs* and *AREB* along the Lineage 2 pseudotime trajectory. **c**, Predicted phosphorylation sites on CaWRKY23/68.

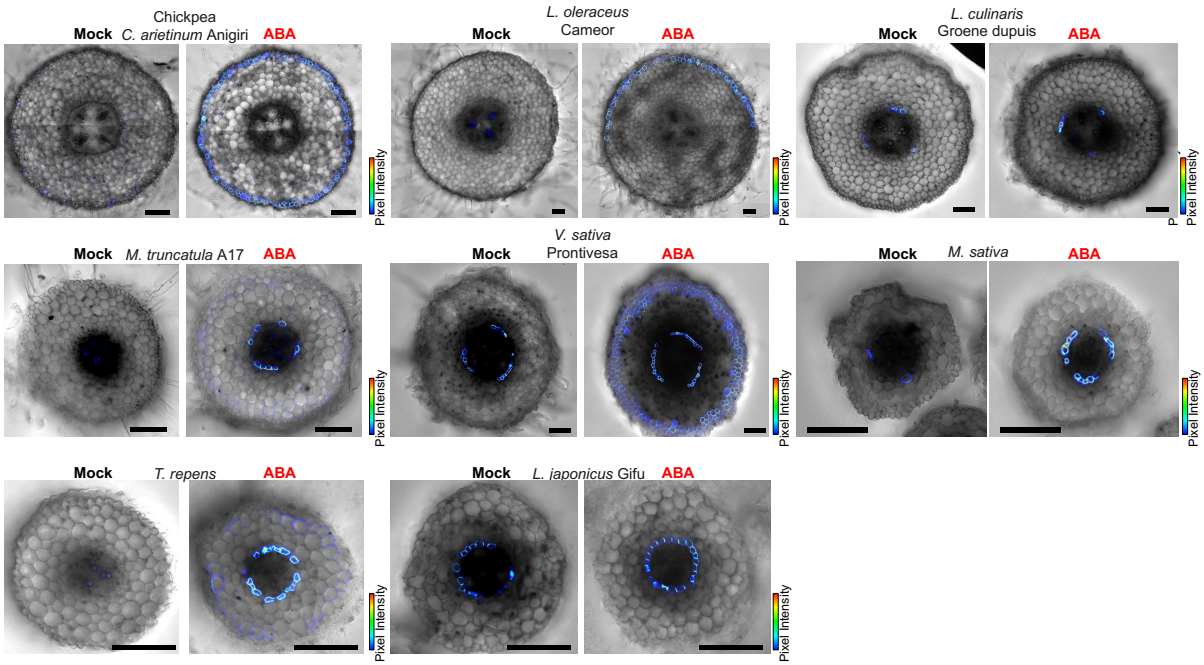

Supplementary Figure 1. Fluorol Yellow staining of root sections.

For each species, representative confocal images of full cross-sections of roots treated with mock or ABA are shown with the FY signal overlaid on top of bright field images (scale bars = 100 µm).

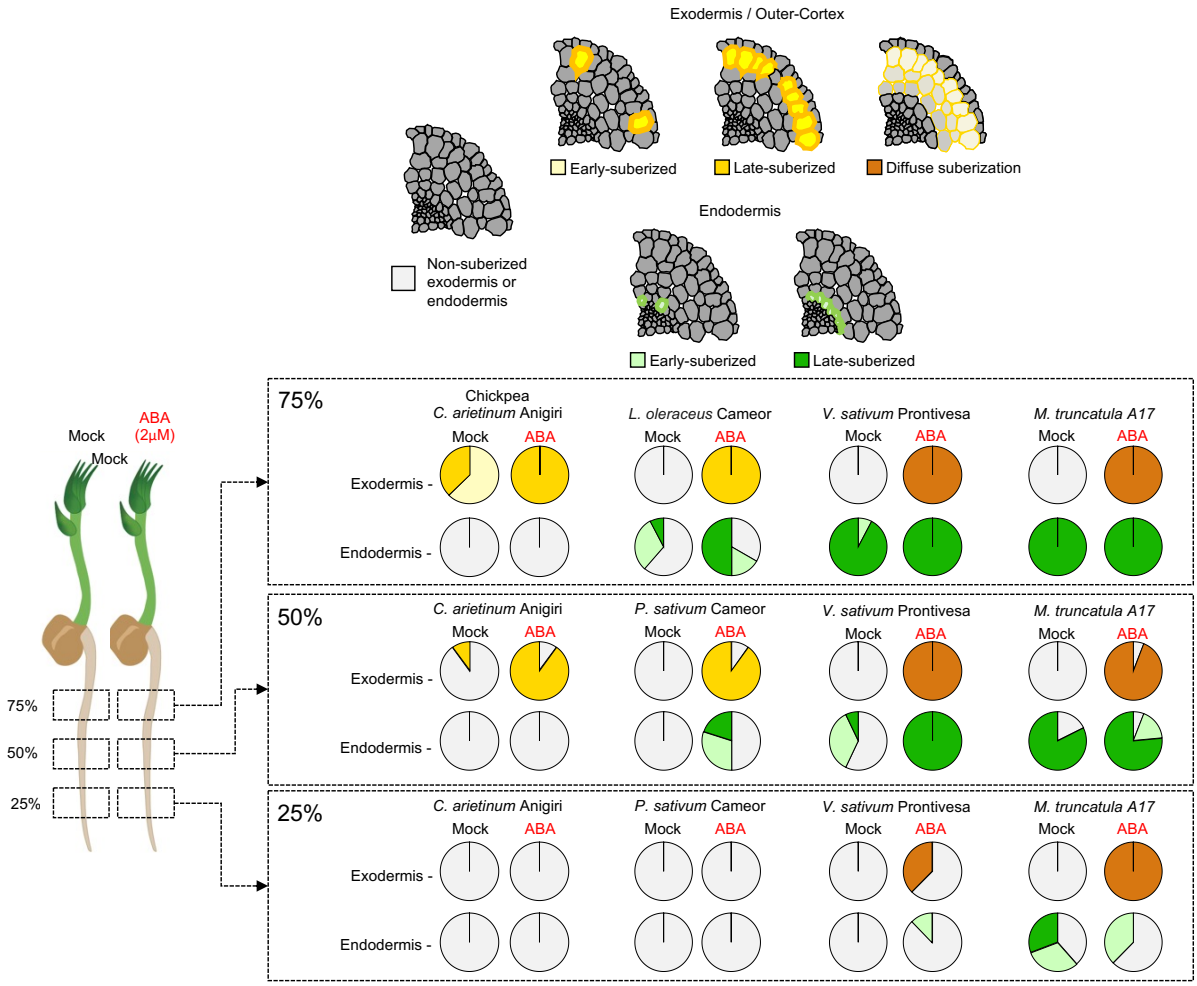

Supplementary Figure 2. Suberin deposition is commonly under developmental and environmental control as shown by its deposition along root developmental zones.

Suberin deposition in distinct developmental zones (25, 50 and 75% region of the root) in the exodermis/outer cortex or endodermis of chickpea (*C. arietinum*), pea (*L. oleraceus*), *V. sativa* and *M. truncatula* roots treated with mock or 2 µM ABA for 3 days. Pie charts depict the percentage of cross sections showing a non-suberized, an early-suberized (suberin in less than 50% of the cells in that layer), a late-suberized (suberin in more than 50% of cells in that layer), or diffuse (weak, non-specific) suberization pattern in the cortex.

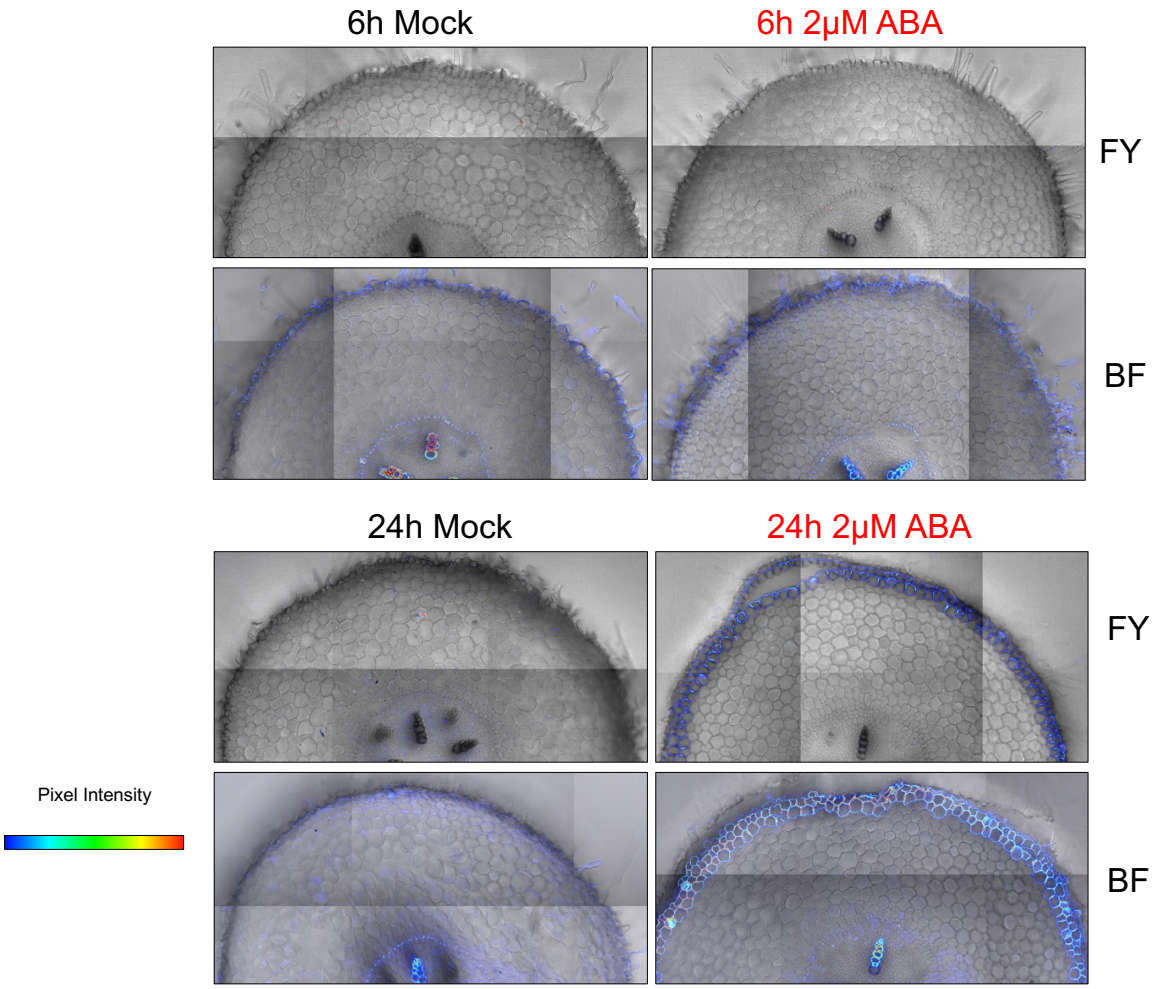

Supplementary Figure 3. Chickpea roots deposit histochemically detectable suberin and lignin in exodermis within 24 h.

Representative confocal images of chickpea roots used for the time course RNA-seq experiment stained with FY and BF are shown. Roots treated with mock or 2 μM ABA at two distinct time points (6 and 24 hours) were cross-sectioned at 75% point as the 50% point shown typically measured was included in the material harvested for RNA-seq. At this developmental zone, additional layer with FY and BF signal can be observed. FY and BF signals are overlaid on top of bright field images. Scale bar = 100 μm.

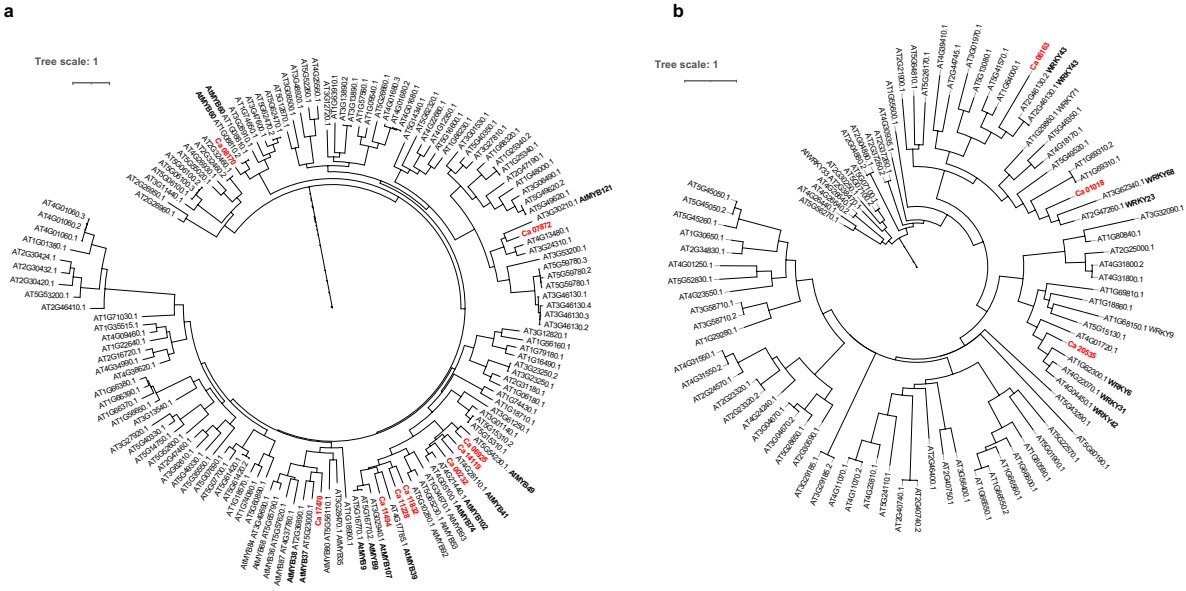

Supplementary Figure 4. CaMYBs and CaWRKYs do not share one-on-one orthology with Arabidopsis TFs.

Representative phylogenetic trees showing the closest Arabidopsis homologs to chickpea **a**, MYBs and **b**, WRKY TFs identified as upregulated by ABA in the time-course bulk RNA-seq experiment. Full length amino acid sequences of chickpea upregulated TFs and all annotated Arabidopsis MYB and WRKY TFs were aligned using MAFFT. The phylogenetic tree was determined using the maximum likelihood method with 1000 bootstraps using iQ-TREE. Distant nodes where chickpea MYB TFs were not detected were removed to improve the visualization of the cladogram. ABA-upregulated *CaMYBs* and *CaWRKYs* are indicated in red, and the TAIR10 symbol respective to close orthologues are indicated.

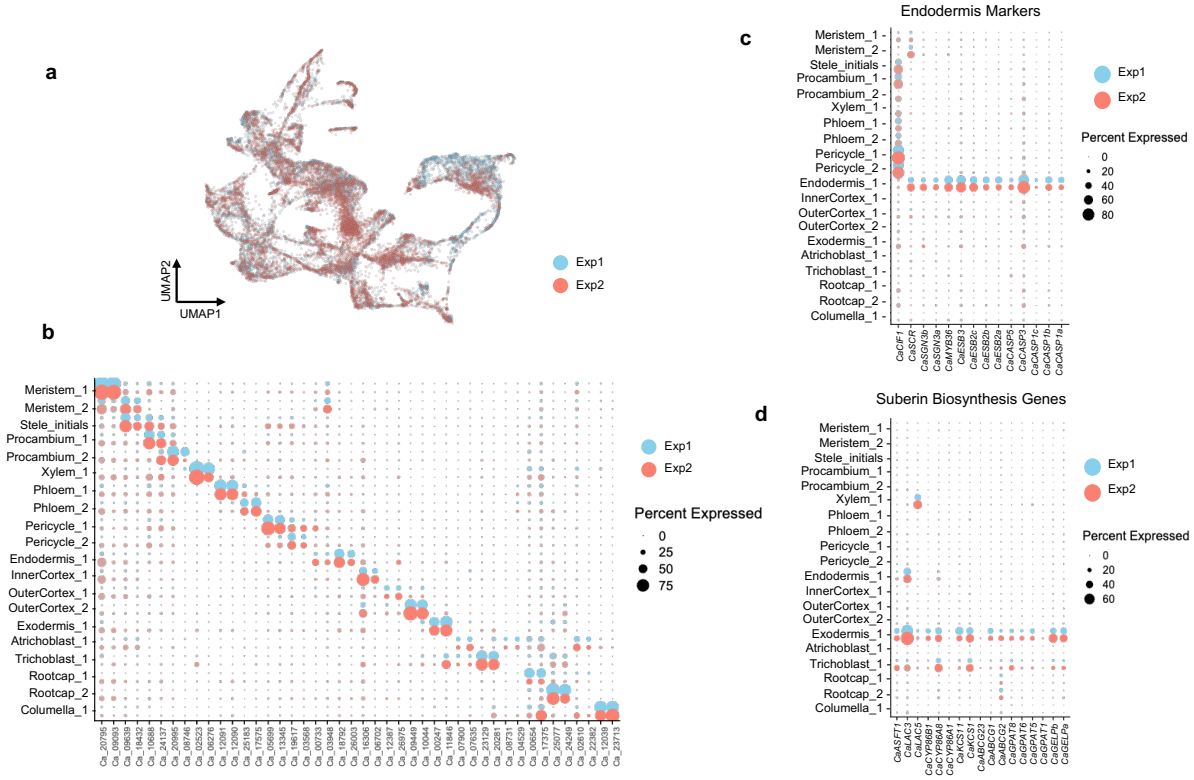

Supplementary Figure 5. Reproducibility of single-cell chickpea root atlas in response to ABA.

Reproducibility as observed by **a,** UMAP. **b**, markers identified, and **c-d,** profile of expression of Casparian strip related genes (**c**) and suberin biosynthesis genes (**d**). Two independent experiments (Exp1 (blue) and Exp2 (salmon)) were carried out that generated independent single-cell libraries. Exp1 used protoplasts isolated from chickpea roots grown in the presence of 2 µM ABA for 24 h, and Exp2 for 48 h. Dot size indicates the percentage of cells in the cluster that expresses the specific gene (% expressed). Dot colors represent the average scaled expression of genes in the clusters (Avg. expression).

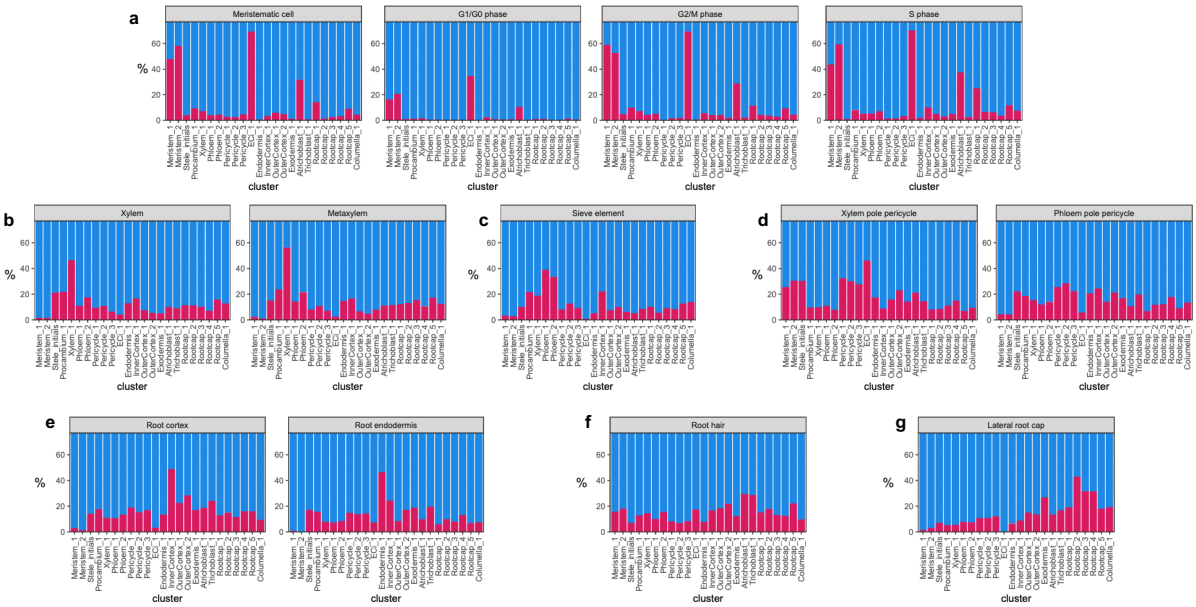

Supplementary Figure 6. Chickpea marker genes in ScPlantDB markers.

Bar plots showing the percentage of chickpea genes in each annotated single-cell cluster that has at least one orthologue identified as a marker in the Arabidopsis root scPlantdb[50] cluster from cell representing **a**, dividing cells, **b**, xylem, **c,** phloem, **d,** pericycle, **e,** ground tissue, **f,** epidermis, and **g**, root cap. We manually curated the datasets in the scPlantdb by only keeping datasets in which *AtMYB36* was annotated as a marker for the endodermal cell cluster.

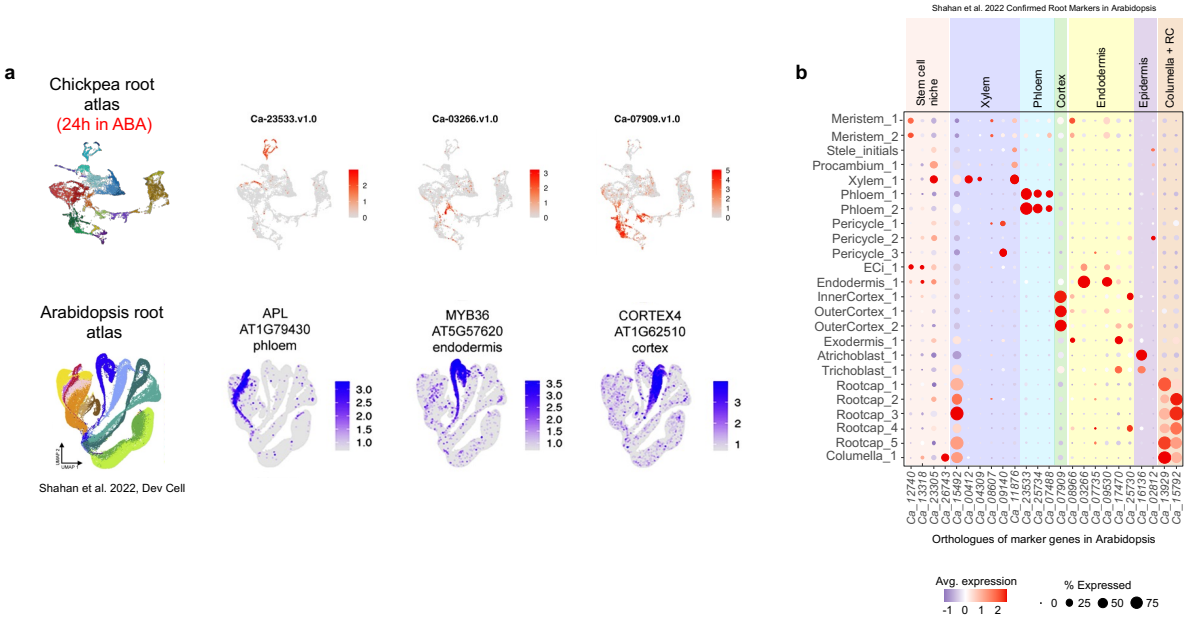

Supplementary Figure 7. Arabidopsis root atlas markers in chickpea single cell data.

a, Top: UMAP profile showing the scaled expression of chickpea orthologue genes to characterized markers in Arabidopsis by [51]. Bottom: UMAP profile showing the scaled expression of marker genes in Arabidopsis phloem, endodermis and cortex[51]. **b**, Dotplot showing the spatial expression of chickpea orthologues of empirically determined root cell markers in Arabidopsis determined by [51].

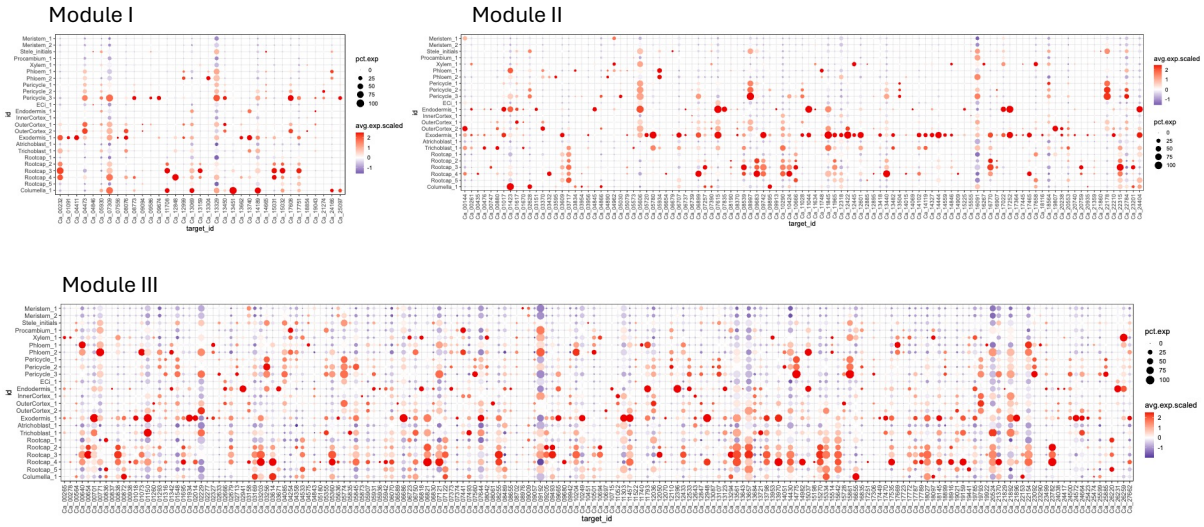

Supplementary Figure 8. Expression of early ABA responsive genes (modules I, II, III) in single cell data.

Dotplot showing the spatial expression of genes found in Modules I, II, and III based on the K-means clustering analysis of the time course bulk-RNAseq experiment in chickpea roots in response to ABA.

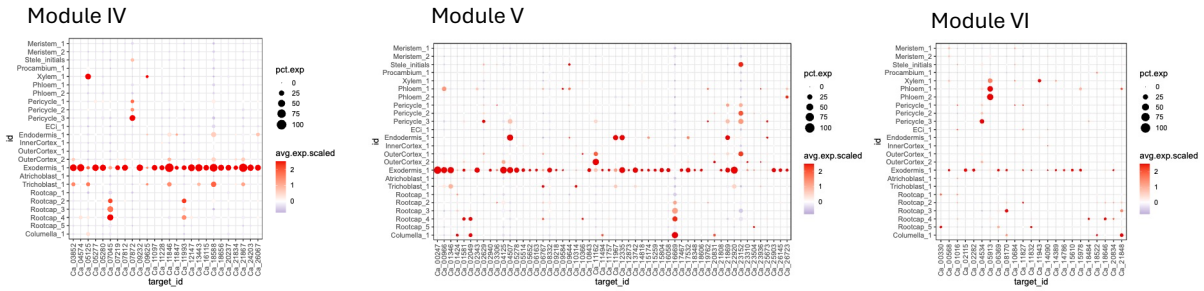

Supplementary Figure 9. Expression of late ABA responsive genes (modules IV, V and VI) in single cell data.

Dotplot showing the spatial expression of genes found in Modules IV, V, and VI based on the K-means clustering analysis of the time course bulk-RNAseq experiment in chickpea roots in response to ABA.

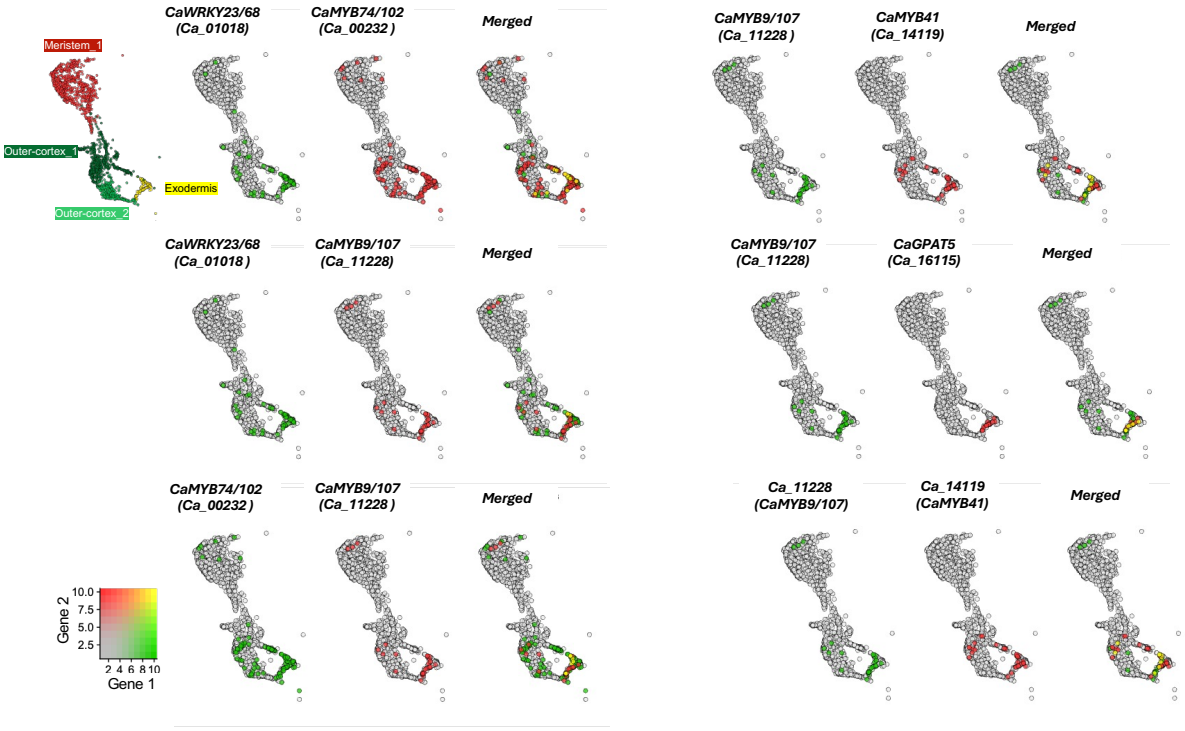

Supplementary Figure 10. Candidate suberin-regulating TFs are often not expressed in the same cells.

Overlap of expression in the single cell clusters representing outer cortex and exodermis for the genes encoding the candidate TFs (*CaWRKY23/68, CaMYB74/102, CaMYB9/107, CaMYB41)* and two suberin biosynthesis genes (*CaGPAT5, CaCYP86B1*). Gene 1 being expressed in a cell (blend threshold of 0.5) in green, gene 2 in red, and both expressed in the same cell in yellow. *CaMYB9/107* was induced by all candidate TFs (Fig. 6e) but it is often not expressed in the same cells as the other candidate TFs.

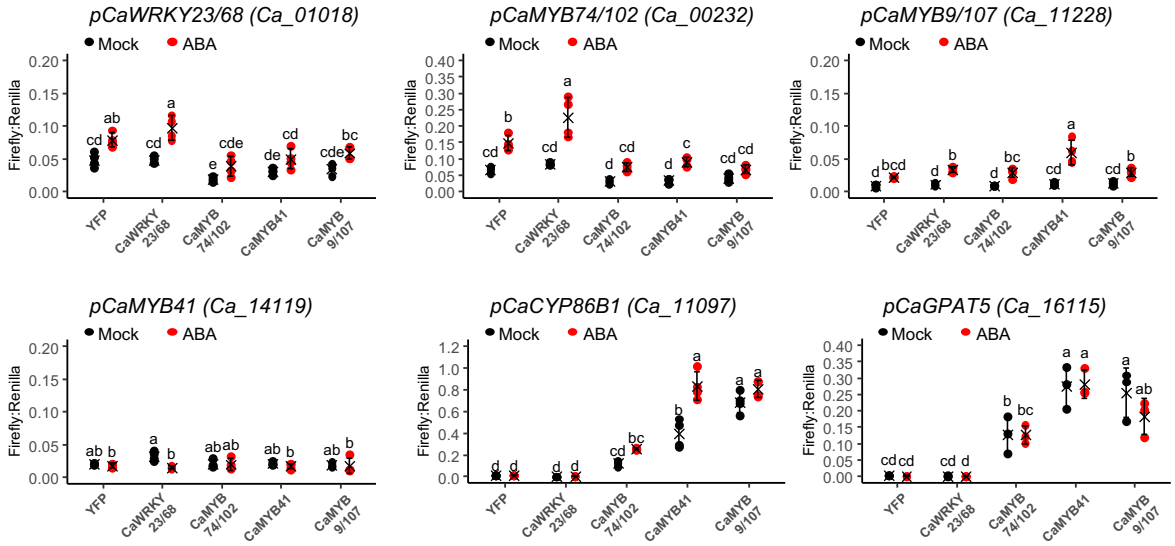

Supplementary Figure 11. Replicate experiments of the transactivation assays.

The transactivation assays (Fig. 6e) were replicated with similar results supporting the same conclusions.